Saccharomyces cerevisiae TORC1 Controls Histone Acetylation by Signaling Through the Sit4/PP6 Phosphatase to Regulate Sirtuin Deacetylase Nuclear Accumulation

Jason J. Workman, Hongfeng Chen, and R. Nicholas Laribee[1]
Department of Pathology and Laboratory Medicine and the University of Tennessee Center for Cancer Research, University of Tennessee Health Science Center, Memphis, Tennessee 38163
ORCID IDs: 0000-0002-9071-5207 (J.J.W.); 0000-0003-4519-4470 (R.N.L.)

ABSTRACT The epigenome responds to changes in the extracellular environment, yet how this information is transmitted to the epigenetic regulatory machinery is unclear. Using a *Saccharomyces cerevisiae* yeast model, we demonstrate that target of rapamycin complex 1 (TORC1) signaling, which is activated by nitrogen metabolism and amino acid availability, promotes site-specific acetylation of histone H3 and H4 N-terminal tails by opposing the activity of the sirtuin deacetylases Hst3 and Hst4. TORC1 does so through suppression of the Tap42-regulated Sit4 (PP6) phosphatase complex, as *sit4Δ* rescues histone acetylation under TORC1-repressive conditions. We further demonstrate that TORC1 inhibition, and subsequent PP6 activation, causes a selective, rapid, nuclear accumulation of Hst4, which correlates with decreased histone acetylation. This increased Hst4 nuclear localization precedes an elevation in Hst4 protein expression, which is attributed to reduced protein turnover, suggesting that nutrient signaling through TORC1 may limit Hst4 nuclear accumulation to facilitate Hst4 degradation and maintain histone acetylation. This pathway is functionally relevant to TORC1 signaling since the stress sensitivity of a nonessential TORC1 mutant (*tco89Δ*) to hydroxyurea and arsenic can be reversed by combining *tco89Δ* with either *hst3Δ*, *hst4Δ*, or *sit4Δ*. Surprisingly, while *hst3Δ* or *hst4Δ* rescues the sensitivity *tco89Δ* has to low concentrations of the TORC1 inhibitor rapamycin, *sit4Δ* fails to do so. These results suggest Sit4 provides an additional function necessary for TORC1-dependent cell growth and proliferation. Collectively, this study defines a novel mechanism by which TORC1 suppresses a PP6-regulated sirtuin deacetylase pathway to couple nutrient signaling to epigenetic regulation.

KEYWORDS target of rapamycin; histone acetylation; Sit4; sirtuins; epigenetic

DYNAMIC chromatin regulation is key to the adaptive mechanisms eukaryotic cells employ to alter cellular phenotype in response to fluctuating environmental conditions, such as changes in nutrient availability and various forms of stress. Environmental regulation of the epigenome profoundly affects health and disease, but how the chromatin regulatory apparatus responds to such influences is not understood (Lu and Thompson 2012; Szyf 2015). A universally conserved signaling pathway regulated by the environment is the target of rapamycin (TOR) pathway (Loewith and Hall 2011; Laplante and Sabatini 2012). TOR consists of two distinct subpathways involving TOR complex 1 (TORC1) and TOR complex 2 (TORC2), of which only TORC1 is activated by environmental inputs (Loewith and Hall 2011; Laplante and Sabatini 2012). In single-celled organisms such as budding yeast, TORC1 is specifically stimulated by the quantity and quality of the available nitrogen source; however, while controversial, recent studies also have suggested potential crosstalk between glucose signaling, carbon metabolism, and TORC1 activation (Schmelzle *et al.* 2004; Soulard *et al.* 2010; Ramachandran and Herman 2011; Dechant *et al.* 2014). Metazoan TORC1 is also regulated by nutrients, specifically amino acids, but requires an additional mitogen/growth factor input for its activation (Laplante and Sabatini

doi: 10.1534/genetics.116.188458
Manuscript received February 19, 2016; accepted for publication June 15, 2016; published Early Online June 22, 2016.
Available freely online through the author-supported open access option.
Supplemental material is available online at www.genetics.org/lookup/suppl/doi:10.1534/genetics.116.188458/-/DC1.
[1]Corresponding author: Cancer Research Bldg., University of Tennessee, 19 S. Manassas, Room 318, Memphis, TN 38163. E-mail: rlaribee@uthsc.edu

2012). TORC1 signaling regulates anabolic processes, including the transcription of genes required for ribosome biogenesis, control of translation, and suppression of catabolic stress responses such as autophagy (Loewith and Hall 2011; Laplante and Sabatini 2012). Given the role TORC1 has in responding to nutrient availability and environmental stress, it is ideally positioned to facilitate information transfer from the environment to the epigenetic regulatory machinery.

Yeast TORC1 consists of either the Tor1 or Tor2 kinase, Kog1, Lst8, and the nonessential subunit Tco89 (Loewith *et al.* 2002; Reinke *et al.* 2004). Loss of either Tor1 or Tco89 causes hypersensitivity to conditions that suppress TORC1 signaling, including nutrient deprivation and the naturally occurring TORC1 inhibitor rapamycin (Loewith and Hall 2011). In yeast, TORC1 resides predominantly on the vacuole's surface where it is activated by luminal amino acid accumulation (Binda *et al.* 2009; Dechant *et al.* 2014). Active TORC1 then signals through at least two well-defined downstream effector pathways. The best characterized is the AGC kinase Sch9, which is directly phosphorylated and activated by TORC1 (Urban *et al.* 2007). Active Sch9 can then phosphorylate a number of distinct substrates, many of which function directly in ribosomal gene transcription and protein translation (Urban *et al.* 2007; Huber *et al.* 2009; Huber *et al.* 2011). A recent study identified the existence of a TORC1 effector pathway distinct from Sch9 involving the Ypk3 kinase, which phosphorylates ribosomal S6, yet this pathway still remains poorly characterized (Gonzalez *et al.* 2015).

In the presence of a high-quality nitrogen source, TORC1 also phosphorylates the essential factor Tap42 (Di Como and Arndt 1996; Jiang and Broach 1999; Yan *et al.* 2012). Phosphorylated Tap42 interacts with the evolutionarily conserved protein phosphatase 2A (PP2A) and PP2A-like phosphatases, which sequesters these enzymes onto the vacuolar surface and restricts their access to client substrates (Di Como and Arndt 1996; Jiang and Broach 1999; Yan *et al.* 2012). Upon nitrogen starvation and reduction of vacuolar amino acids, Tap42-regulated phosphatase complexes are released that then dephosphorylate several key transcription factors, including Gln3 and Gat1 (Beck and Hall 1999; Kuruvilla *et al.* 2001; Crespo *et al.* 2002). Dephosphorylation triggers Gln3 and Gat1 dissociation from their cytoplasmic anchor Ure2 and their subsequent nuclear translocation. Nuclear Gln3 and Gat1 then regulate transcription of genes involved in the metabolism of nonpreferred nitrogen sources as part of the nitrogen catabolite repression (NCR) response (Cooper 2002). Each of the Tap42-regulated phosphatases consists of a defining catalytic subunit, as well as additional regulatory subunits that elicit distinct regulatory functions. For example, the catalytic subunit of the PP6 phosphatase complex, Sit4, forms heterodimers with one of four regulatory subunits (Sap4, Sap155, Sap185, or Sap190) that direct its enzymatic activity to specific substrates involved in cell-cycle regulation, transcription, and translation (Luke *et al.* 1996; Rohde *et al.* 2004).

Recently, TORC1 has also been implicated in the regulation of chromatin structure through control of histone post-translational modifications. For example, TORC1-dependent transcription of ribosomal protein gene expression was demonstrated to require the Esa1 histone acetyltransferase, which acetylates histone H4 (Rohde and Cardenas 2003). TORC1 suppression was also shown to cause rapid histone deacetylation of ribosomal DNA (rDNA) repeats and increased transcriptional silencing via recruitment of the sirtuin deacetylase Sir2 (Ha and Huh 2011). Our group recently demonstrated that TORC1 regulates global histone H3 lysine 56 acetylation (H3K56ac) to facilitate ribosomal RNA synthesis by RNA polymerase I through a pathway connected to the sirtuins Hst3 and Hst4 (Chen *et al.* 2012). However, the relationship between TORC1 signaling and these sirtuins was not defined in detail. A subsequent study demonstrated that TORC1 signaling causes rDNA repeat expansion, while decreased TORC1 activity reduces rDNA repeat number through a mechanism requiring Sir2, Hst3, and Hst4 (Jack *et al.* 2015). Sirtuin deacetylases are a family of class III NAD^+-dependent deacetylases whose catalytic activities are inversely regulated by energy state (Imai and Guarente 2014). Interestingly, in metazoans, TORC1 signaling and sirtuin activity also are regulated in an opposing fashion (Ghosh *et al.* 2010; Guo *et al.* 2011; Csibi *et al.* 2013). Therefore, these studies suggest that TORC1 signaling and sirtuin activity may be coordinated in opposing ways to link control of epigenetic changes needed for anabolism with the availability of environmental nutrients to support these processes.

In this report, we expand on these concepts to demonstrate that nitrogen availability signals through TORC1 to regulate site-specific acetylation of select histone H3 and H4 N-terminal lysine residues besides H3K56ac. We demonstrate that TORC1 controls these modifications globally via repression of Tap42-regulated Sit4 phosphatase activity. TORC1 suppression promotes a decrease in histone acetylation, which requires the activation of Sit4 and the sirtuins Hst3 and Hst4. Specifically in the case of Hst4, reduced TORC1 activity increases Hst4 nuclear localization and reduces Hst4 protein turnover, suggesting that Hst4 nuclear localization may stabilize the enzyme to mediate histone deacetylation under nutrient-limiting conditions. This TORC1-dependent suppression of Sit4/PP6 and downstream negative regulation of sirtuins is biologically relevant as deletions of Sit4, Hst3, or Hst4 rescue some TORC1 mutant phenotypes.

Materials and Methods

Yeast plasmids, strains, and culture conditions

The strains and plasmids utilized are listed in Supplemental Material, Table S1 and Table S2, respectively. Gene deletion and epitope tagging procedures were conducted as described previously (Janke *et al.* 2004). Unless explicitly stated, all yeast cultures and plating assays were performed in 1% yeast extract/2% peptone/2% dextrose (YPD). Yeast drop-out

synthetic complete (SC) media were prepared as described previously (Laribee *et al.* 2015). All yeast culture media were purchased from US Biologicals and Research Products International, and antibiotics for selection were obtained from Invitrogen (Carlsbad, CA) or GoldBio. Cells were cultured either at 30° or room temperature (for the *tap42ts* experiments) with shaking. For the spotting assays, equal cell numbers from overnight cultures were pelleted, washed, and serially diluted fivefold. Cells were then spotted to the appropriate plates, incubated at the indicated temperatures, and photographed daily. Full-length *TCO89* or *SIT4* open reading frames were cloned in-frame as C-terminal mono-FLAG fusions into the *Bam*HI/*Xba*I (*TCO89-FLAG*) or *Bam*HI/*Eco*RI (*SIT4-FLAG*) restriction sites of plasmid p416ADH, which contains an *ADH1* promoter and *CYC1* terminator sequence (Mumberg *et al.* 1995).

Stains and antibodies

The antibodies used are as follows: α-RPS6 (Abcam), α-phosphoS6 (Cell Signaling), α-FLAG (Stratagene, La Jolla, CA), goat α-rabbit HRP-conjugated secondary (The Jackson Laboratory), α-HA and α-Myc A14 (Santa Cruz Biotechnology), α-G6PDH (Sigma, St. Louis, MI), α-FLAG (ThermoFisher), and goat α-rabbit FITC-conjugated secondary (Rockland). All histone antibodies were purchased from Active Motif. For confocal microscopy, Vectashield mounting media containing DAPI were purchased from Vector Laboratories (Burlingame, CA).

RT-quantitative PCR, statistical analyses, and immunoblot analyses

Total RNA was extracted and 1 μg of DNase I digested RNA was used to synthesize randomly primed complementary DNA (cDNA) using the ImProm II reverse transcription system from Promega (Madison, WI). Gene-specific quantitative PCR (qPCR) with normalization to the *SPT15* housekeeping gene was performed and analyzed as previously described (Laribee *et al.* 2015). Primer sequences are available upon request. All statistical analyses reported in this study were performed using Student's *t*-test and the statistical suite available in Microsoft Excel. Whole-cell extracts were prepared and immunoblotting was performed as outlined previously (Laribee *et al.* 2015). To quantify histone immunoblot results, films were scanned and analyzed by ImageJ software. Histone acetylation states were always normalized to total histone H3 levels to account for any variability in histone levels.

Indirect immunofluorescence confocal microscopy

Small scale cultures (10 ml) were cultured to log phase and treated as indicated. The cells were then fixed with 37% formaldehyde, pelleted, and washed twice with 0.1 M potassium phosphate buffer (K_2HPO_4, pH = 6.5) and once with 4 ml P solution (1.2 M sorbitol, 0.1 M K_2HPO_4, pH = 6.5). Pellets were resuspended in 1 ml P solution, 15 μl LongLife Zymolase (15 mg/ml in P solution) and 5 μl β-mercaptoethanol, followed by a 25-min incubation with gentle mixing at room temperature. After zymolase treatment, cells were pelleted, resuspended in 150 μl of P solution, and distributed evenly across two hydrophobic barrier regions of a polylysine-coated microscope slide. Cells were allowed to settle prior to blocking (8% bovine serum albumin, 0.5% Tween 20 in PBS for 20 min). Blocking solution was removed and primary antibody (1:100 α-Myc) was added for a humidified incubation overnight at 4°. Slides were washed four times with blocking solution and then incubated with FITC-conjugated secondary antibody (1:100) for 60 min at room temperature. The slide washes were repeated four times with blocking solution, twice with PBS, and then a drop of DAPI-containing Vectashield mounting medium was added before coverslip addition and sealing.

Image analysis in Zen 2 Blue

Image quantification was performed using Zen 2 Blue Lite, version 2.0.0 software. Two borders were traced onto the image using the Spline Contour tool, one around the cell periphery and the other around the nucleus. After closing each border, values were obtained for the area encompassed by the border, as well as the mean intensity value for each channel inside that space. The area within the nuclear border was multiplied by the mean intensity value for the green channel (FITC-conjugated secondary fluorescence green). This gave a number for the total nuclear fluorescence intensity (TNFI):

$$\text{TNFI} = \text{nuclear area } (\text{nm}^2) \times \text{nuclear mean intensity value}.$$

This same calculation was repeated using the outer cell border values, providing us a measure of the total cellular fluorescence intensity (TCFI):

$$\text{TCFI} = \text{cellular area } (\text{nm}^2) \times \text{cellular mean intensity value}.$$

We then performed the following calculation to get the percentage of nuclear protein:

$$\%\text{nuclear} = \text{TNFI}/\text{TCFI} \times 100.$$

Cells were chosen for analysis at random, with ~20–40 quantified per condition, per biological replicate (four to six replicates). Only cells with clear nuclear DNA staining and detectable α-Myc signal were quantified. For the immunostaining, cells whose cellular mean intensity was <50 units were considered to have not been penetrated by secondary antibody and were excluded from calculations.

Protein turnover analysis

Myc-tagged Hst3 or Hst4 strains were cultured to log phase in 200 ml YPD media. The 50-ml samples were sterilely retrieved from each flask prior to cycloheximide (CHX) addition (100 μg/ml). Following treatment, additional 50-ml

aliquots were taken at the time points indicated. Whole-cell extracts were prepped and analyzed by SDS/PAGE and α-Myc immunoblot. Films were scanned and Hst3 or Hst4 levels were normalized to total protein (G6PDH) levels by ImageJ analysis.

Data availability

The authors state that all data necessary for confirming the conclusions presented in the article are represented fully within the article.

Results

Metabolic signaling through TORC1 regulates site-specific histone H3 and H4 acetylation

Previously, we demonstrated that TORC1 signaling regulates global H3K56ac (Chen *et al.* 2012). We wanted to assess whether this effect was unique for H3K56ac, or if TORC1 also contributed to the regulation of other histone H3 and H4 acetyl modifications as well. To explore this possibility, we performed immunoblot analysis for site-specific histone H3/H4 N-terminal acetylation modifications. Duplicate wild-type (WT) cultures, as well as a *tco89Δ* (nonessential TORC1 subunit), were cultured to log phase and either mock treated or treated with 300 nM rapamycin for 60 min before preparing whole-cell extracts. The concentration and length of rapamycin treatment chosen was confirmed to inhibit TORC1 signaling via phosphoS6 analysis (Figure S1A). Immunoblot analysis identified H3K18ac, H3K23ac, and H4K12ac to be selectively decreased after TORC1 inhibition, whereas all other acetylation states were unaffected (Figure 1, A and B). Furthermore, this effect was not due to globally reduced transcription-coupled histone modifications, as histone H3 lysine 4 trimethylation (H3K4me3), which demarcates transcriptionally active genes, was unaffected (Figure 1A). These changes occurred rapidly as WT cells treated with 200 nM rapamycin for 20 min displayed profoundly reduced global H3K18ac (Figure S1B). Importantly, restoration of WT Tco89 expression in *tco89Δ* cells completely rescued histone acetylation, thereby demonstrating that the reduced acetylation were solely due to impaired TORC1 activity (Figure 1C).

Nitrogen metabolism and amino acid availability are known activators of TORC1 (Beck and Hall 1999; Cardenas *et al.* 1999; Hardwick *et al.* 1999; Crespo *et al.* 2002). Intriguingly, carbon metabolism has also recently been suggested to activate TORC1 through the vacuolar localized V-ATPase complex, while glycolysis is known to control global levels of many of the same histone acetylation sites we have identified to be regulated by TORC1 (Friis *et al.* 2009; Dechant *et al.* 2014). Therefore, we next determined the impact these distinct nutrient signals have on TORC1-regulated acetylation. Changing the carbon source from glucose to a nonfermentable carbon (glycerol) failed to decrease histone acetylation in WT cells, nor did it suppress the acetylation defect observed in the *tco89Δ* mutant (Figure 1D). Because cells grow considerably slower in the presence of a nonfermentable carbon, these results also exclude the possibility that the difference in acetylation between WT and *tco89Δ* is caused by a reduced growth rate in *tco89Δ*. To assess the contribution of nitrogen metabolism, we cultured WT cells to log phase and mock treated or treated cells for 20 min with 2 mM L-methionine sulfoximine (MSX) to inhibit glutamine synthetase, thus mimicking a nitrogen starvation state. MSX rapidly decreased H3K18ac (Figure 1E, top panel, and F), which we confirmed also suppressed TORC1 activity (Figure 1E, bottom panel). These data demonstrate that nitrogen-, but not carbon-dependent TORC1 activation is responsible for regulating these site-specific histone acetylation states.

TORC1 signaling through the Tap42-Sit4/PP6 phosphatase is required for global site-specific histone acetylation

TORC1 activates multiple downstream effectors, including the Sch9 kinase, which is directly phosphorylated by TORC1 (Urban *et al.* 2007). To determine if TORC1 regulates histone acetylation through Sch9 activation, we utilized a series of previously described Sch9 plasmids including $Sch9^{WT}$, $Sch9^{5A}$, in which the TORC1 target sites are mutated to alanine to mimic the nonphosphorylated form, and $Sch9^{2D3E}$, in which the TORC1 target sites are mutated to acidic residues, rendering it active independent of TORC1 (Urban *et al.* 2007). Critically, we found that these various mutant forms had similar expression and stability (Figure S2A). Additionally, we confirmed that in *sch9Δ*, the $Sch9^{2D3E}$ plasmid promoted growth on nonfermentable carbon and rapamycin as expected (Figure S2B) (Urban *et al.* 2007). We also confirmed that in a *sch9Δ* + $pSch9^{2D3E}$ strain, Maf1 phosphorylation (a direct substrate of Sch9) was maintained after rapamycin inhibition (Figure S2C) (Huber *et al.* 2009; Wei and Zheng 2009), all together demonstrating that $Sch9^{2D3E}$ functioned as expected. However, *tco89Δ* cells expressing $Sch9^{2D3E}$ failed to rescue histone acetylation (Figure 2A). Similarly, a *sch9Δ* strain did not reduce histone acetylation (Figure 2B), thus demonstrating that TORC1-dependent acetylation is regulated independently of Sch9.

Next, we asked whether TORC1 signaled through its other downstream effector, Tap42, to regulate histone acetylation. *TAP42* is an essential gene, so we utilized *tap42Δ* cells containing a plasmid expressing either WT or temperature-sensitive (*ts*) *tap42* alleles (Yorimitsu *et al.* 2009). We confirmed the temperature sensitivity of these strains and chose *tap42-106* for further analysis because it exhibited the least growth inhibition at 30° (Figure 2C). As a consequence, it would be less likely to have nonspecific effects on acetylation due to loss of viability. WT and *tap42-106* cells were cultured to log phase at permissive (25°) temperature before being shifted to 30° for 1 hr. Even at room temperature, where there is no evident growth phenotype (Figure 2C), the *tap42-106* mutant exhibited significant H3K18ac reduction, thus implicating Tap42 in histone acetylation regulation (Figure 2, D

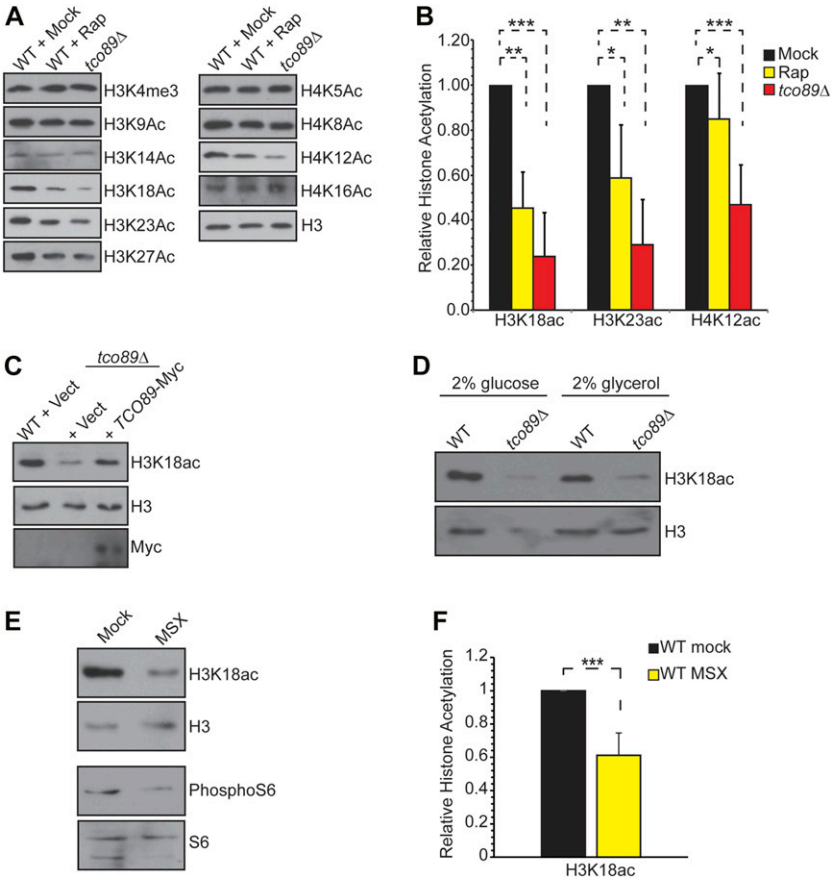

Figure 1 Nitrogen signaling through TORC1 regulates site-specific histone acetylation. (A) WT and *tco89Δ* strains were cultured to log phase and WT cells were then mock treated or treated with 300 nM rapamycin for 1 hr before harvesting. Whole-cell extracts were then analyzed by immunoblot (IB) with the indicated antibodies. α-H3 is included as the loading control for the panel. (B) Quantification of the results from A. Data are the average and SD of a minimum of four or more independent experiments and significance was determined by Student's *t*-test. * $P < 0.05$; ** $P < 0.01$; *** $P < 0.001$. (C) WT and *tco89Δ* were transformed with control vector or a *TCO89-9xMyc* expression vector. Log phase cells were harvested and analyzed by IB with the indicated antibodies. (D) WT and *tco89Δ* cells were cultured to log phase in YPD (2% glucose) or YPGly (2% glycerol) before preparing cell extracts and IB analysis. (E) WT cells were cultured to log phase and then mock treated or treated with 2 mM MSX for 20 min before harvesting and analyzing H3K18ac and phosphoS6 by IB. (F) Quantification of acetylation results from E. Data are the average and SD of nine independent experiments. Significance was determined as in B.

and E). Importantly, the decreased acetylation was specific for H3K18ac, as H3K9ac, which is not affected by TORC1 inhibition, was intact (Figure 1A and Figure 2D). At the more restrictive (30°) temperature, *tap42-106* caused an even greater reduction in H3K18ac without affecting H3K9ac (Figure 2, D and E). Taken together, these results demonstrate that TORC1 signals through a Tap42-dependent phosphatase pathway to regulate site-specific histone acetylation.

TORC1-dependent Tap42 phosphorylation allows Tap42 to interact with PP2A and PP2A-like phosphatase (PP'ase) complexes, which promotes their sequestration to the vacuole surface and restricts their access to substrates (Di Como and Arndt 1996; Jiang and Broach 1999; Yan *et al.* 2012). To identify which candidate PP'ase is required for TORC1-regulated acetylation, we screened deletion mutants of individual catalytic PP'ase subunits (PPG1/*ppg1Δ*, PP4/*pph3Δ*, and PP6/*sit4Δ*) for the loss of rapamycin-induced deacetylation. Since two redundant catalytic subunits exist for PP2A (Pph21 and Pph22), we instead examined a *tpd3Δ*, which eliminates the PP2A regulatory subunit and impairs PP2A activity (Hombauer *et al.* 2007). TORC1 inhibition suppressed H3K18ac, as well as H3K56ac, which we previously identified to be TORC1 dependent, in WT cells and all mutants examined except for *sit4Δ* (Figure 3A and data not shown).

To confirm the Sit4-catalyzed PP6 phosphatase complex was indeed responsible for TORC1-dependent acetylation, WT and *sit4Δ* cells were reconstituted with control vector or a vector expressing a Sit4–FLAG construct. In control vector containing *sit4Δ* cells, higher basal H3K18ac levels were detected that were insensitive to rapamycin, while *sit4Δ* expressing WT Sit4 reduced H3K18ac and restored rapamycin-dependent acetylation repression (Figure 3B). We also confirmed that *sit4Δ* alone increased basal H3K18ac while a *tco89Δ sit4Δ* restored H3K18 acetylation to near WT levels relative to *tco89Δ* (Figure 3C). These results suggest that Sit4 mediates active repression of histone acetylation under limited TORC1 signaling conditions. As Sit4 partners with one of four different Sap (Sit4-associated protein) regulatory subunits to target distinct substrates, we utilized the same approach from Figure 3A to evaluate the contributions of these ancillary subunits to acetylation regulation. Interestingly, we determined that no single SAP deletion is sufficient to restore WT H3K18 acetylation (compare to the effect of *sit4Δ* in Figure 3A), although the most significant rescue is observed in the *sap4Δ* and *sap185Δ* strains (Figure 3D). This suggests the possibility that these Saps have some functional redundancy as has been suggested previously (Rohde *et al.* 2004).

The best characterized Sit4 function is in the regulation of the NCR response (Beck and Hall 1999; Crespo *et al.* 2002). Because nitrogen signaling through TORC1 regulates histone acetylation in a Sit4-dependent fashion, we probed whether Sit4 mediated this effect through activation of the NCR gene expression program. Surprisingly, while Sit4 loss significantly upregulated basal H3K18ac levels as expected, we

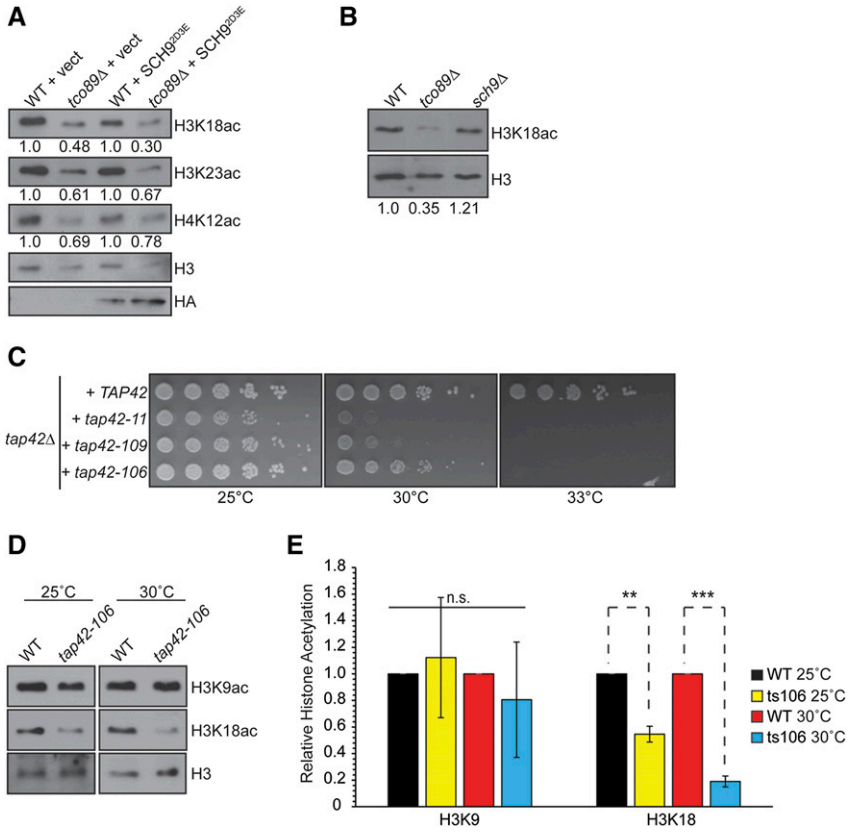

Figure 2 Tap42, not Sch9, is the TORC1 downstream effector promoting changes in histone acetylation states. (A) WT and *tco89Δ* cells were transformed with control vector or an SCH9^{2D3E}-HA expression vector and cultured to log phase before harvesting and analyzing acetylation by IB and ImageJ as indicated. An α-HA blot is included as control for Sch9^{2D3E} expression. Data are representative of at least three independent replicates, and mean histone acetylation values (relative to H3 with WT set to 1) are provided below the corresponding panel. (B) WT, *tco89Δ*, and *sch9Δ* cells were cultured to log phase before harvest. Four independent sets of extracts were analyzed by IB and ImageJ as described in A. (C) *tap42Δ* mutants expressing plasmid-borne *TAP42* or the indicated *tap42ts* mutants were cultured overnight to saturation. Equal numbers of cells were serially diluted fivefold, spotted onto YPD plates, and incubated either at room temperature (permissive), 30° (semipermissive), or 33° (nonpermissive) for 2 days before photographing. (D) *TAP42* WT and *tap42-106ts* strains were cultured to log phase at room temperature before heat shocking at 30° for 1 hr. Cells were then harvested and analyzed with the indicated antibodies. (E) Quantification of results from D. Data in E are the average and SD of three independent experiments and significance was determined by Student's *t*-test. * $P < 0.05$; ** $P < 0.01$; *** $P < 0.001$.

determined that neither deletion of the transcription factors Gln3 and Gat1, nor their cytoplasmic anchor Ure2, resulted in a similar increase in acetylation (Figure 3E). These findings demonstrate that while the Sit4-catalyzed PP6 phosphatase complex specifically represses acetylation under TORC1 limiting conditions, it does so independently of the NCR pathway.

TORC1 opposes sirtuin deacetylase function to promote histone acetylation in a site-specific fashion

We next tested whether TORC1-dependent acetylation involved sirtuin deacetylases since we previously identified a connection between TORC1 and sirtuins in H3K56ac regulation (Chen *et al.* 2012). Initially, we cultured WT and *tco89Δ* cells to log phase and either mock treated or treated with the pan-sirtuin inhibitor nicotinamide before analyzing acetylation. Basal H3K18ac increased in nicotinamide-treated WT cells, suggesting a role for sirtuins in regulating global steady-state acetylation levels, while nicotinamide completely restored acetylation in *tco89Δ* (Figure 4A). Additionally, treating log phase WT and *tco89Δ* cultures with the inhibitor FK866, which inhibits nicotinamide phosphoribosyltransferase to suppress NAD^+ biosynthesis and inactivate sirtuins, completely restored acetylation in *tco89Δ* (Figure 4B) (Hasmann and Schemainda 2003). TORC1 actively suppresses transcription of the *PNC1* gene, which encodes a nicotinamidase that degrades nicotinamide to nicotinic acid as part of the NAD^+ salvage pathway (Medvedik *et al.* 2007). Therefore, one possible link between TORC1 suppression and reduced histone acetylation could be increased Pnc1 enzymatic activity, which would reduce nicotinamide levels to consequently activate sirtuins. Surprisingly, combining *tco89Δ* with a *pnc1Δ* failed to restore histone acetylation, demonstrating that TORC1 suppression does not reduce histone acetylation by upregulating *PNC1* gene expression (Figure 4C). Collectively, these results demonstrate that TORC1 suppression reduces histone acetylation through a Sit4 and sirtuin-dependent pathway, but it does so independently of changes to the NAD^+ biosynthetic pathway known to activate sirtuins.

To test whether the decrease in acetylation downstream of TORC1 inhibition might additionally involve class I and II histone deacetylases, we combined *tco89Δ* with a deletion in either the major class I or class II deacetylase (*rpd3Δ* and *hda1Δ*, respectively) known to regulate transcription and then analyzed whether inactivating either of these enzymes restored histone acetylation (Rundlett *et al.* 1996). Although basal acetylation was increased at our TORC1-responsive sites (K18ac and K23ac) in both the *rpd3Δ* and *hda1Δ* cells, the *tco89Δ rpd3Δ* and *tco89Δ hda1Δ* still displayed diminished acetylation, thus confirming that TORC1 acts independently of major class I or class II deacetylases to control global histone acetylation states (Figure 4D). Five sirtuins (Hst1, Hst2, Hst3, Hst4, and Sir2) exist in yeast (Wierman and Smith 2014). To identify which specific sirtuin(s) are connected to the TORC1 pathway, we generated combinatorial mutants of *tco89Δ* paired with deletions of the individual

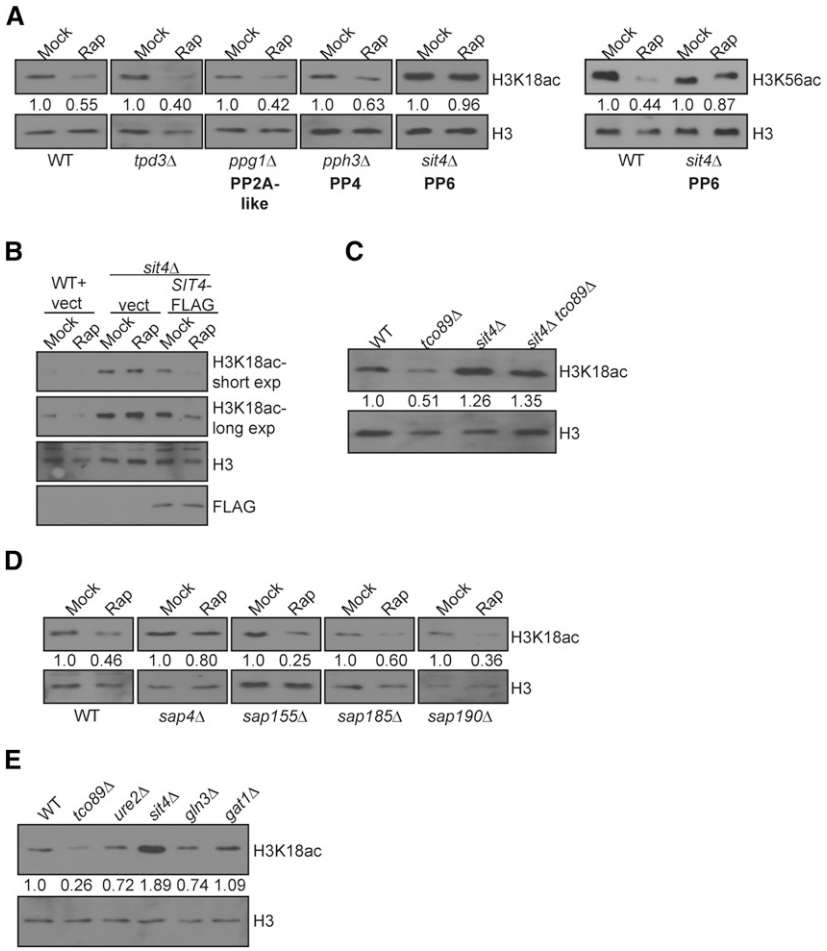

Figure 3 The Tap42–Sit4 PP6 phosphatase complex is necessary for TORC1-dependent chromatin changes. (A) WT and the indicated PP'ase mutants were cultured to log phase and then mock or 300 nM rapamycin treated for 1 hr before harvesting and performing IB and ImageJ analysis with the indicated antibodies. (B) WT and *sit4Δ* cells were transformed with control vector or a *SIT4-FLAG* expression vector and the rapamycin experiment from A was repeated. Both a short and long exposure of the H3K18ac IBs are provided for clarity. (C) WT, *sit4Δ*, *tco89Δ*, and *tco89Δ sit4Δ* cells were cultured to log phase before preparing cell extracts and analyzing by IB as in A. (D) As in A except individual deletions of the Sap-encoding genes were probed. (E) WT, *tco89Δ*, *ure2Δ*, *sit4Δ*, *gln3Δ*, and *gat1Δ* cells were cultured to log phase and whole-cell extracts were analyzed by IB and ImageJ with the indicated antibodies. Blots and mean acetylation data relative to H3 (mock set to 1) presented in A–E are representative of at least four independent experiments.

sirtuins and analyzed global histone acetylation. Each double mutant resulted in a unique array of acetylation changes, but only the *tco89Δ hst4Δ* restored H3K18ac, H3K23ac, and H4K12ac to near WT levels (Figure 4, E and F). These data are consistent with our previous finding that *hst3Δ* or *hst4Δ* restores H3K56ac in *tco89Δ* and suggest that TORC1-dependent regulation of site-specific H3/H4 N-terminal acetylation requires repression of PP6 activity and downstream suppression of sirtuin deacetylases, particularly Hst4.

TORC1 regulates Hst4 cellular localization and stability

Recently, inhibition of the mammalian TORC1 (mTORC1) complex was demonstrated to induce transcriptional upregulation of *SIRT4* to promote glutamine anaplerosis (Csibi *et al.* 2013). We next assessed if the Hst4-dependent decrease in histone acetylation upon TORC1 inhibition could be explained by increased Hst4 expression. To address this, we integrated a 9xMyc epitope at the *HST4* genomic locus in WT and *tco89Δ* backgrounds, and then cells were either mock treated or treated with MSX or rapamycin for the indicated times. No significant difference in Hst4 levels was detected in WT cells treated for 20 min with either MSX or rapamycin; however, both *tco89Δ* and WT cells treated with rapamycin for 60 min displayed increased Hst4 protein levels compared to the mock-treated WT control (Figure 5A and Figure S3). These results were surprising since we previously determined that 20 min of rapamycin or MSX treatment was sufficient to effectively decrease histone acetylation (Figure 1E and Figure S1B), yet Hst4 protein levels do not increase until much later after TORC1 suppression. We evaluated the other sirtuins in response to TORC1 inhibition and found that only Sir2 protein was similarly elevated (Figure S3). However, Sir2 is unlikely to contribute to the decrease in histone acetylation upon TORC1 limitation, since a *tco89Δ sir2Δ* mutant failed to restore TORC1-responsive histone acetylation (Figure 4, E and F).

To ascertain whether Sit4 contributes to the regulation of Hst4 protein expression, we generated *sit4Δ* and *tco89Δ sit4Δ* strains in the Hst4-9xMyc background and examined Hst4 levels. While *tco89Δ* increases Hst4 expression, the *sit4Δ* dramatically reduced Hst4 levels relative to WT (Figure 5B). Intriguingly, the *sit4Δ tco89Δ* returned Hst4 expression to WT levels, suggesting that TORC1 acts to repress PP6 activity and limit Hst4 protein expression (Figure 5B). When the experiment was repeated in a *sap4Δ* background, which is the regulatory subunit that most robustly restored histone acetylation in response to rapamycin (Figure 3D), we observed a comparably modest effect on Hst4 protein levels (Figure 5B). These findings are in line with the possibility that some functional

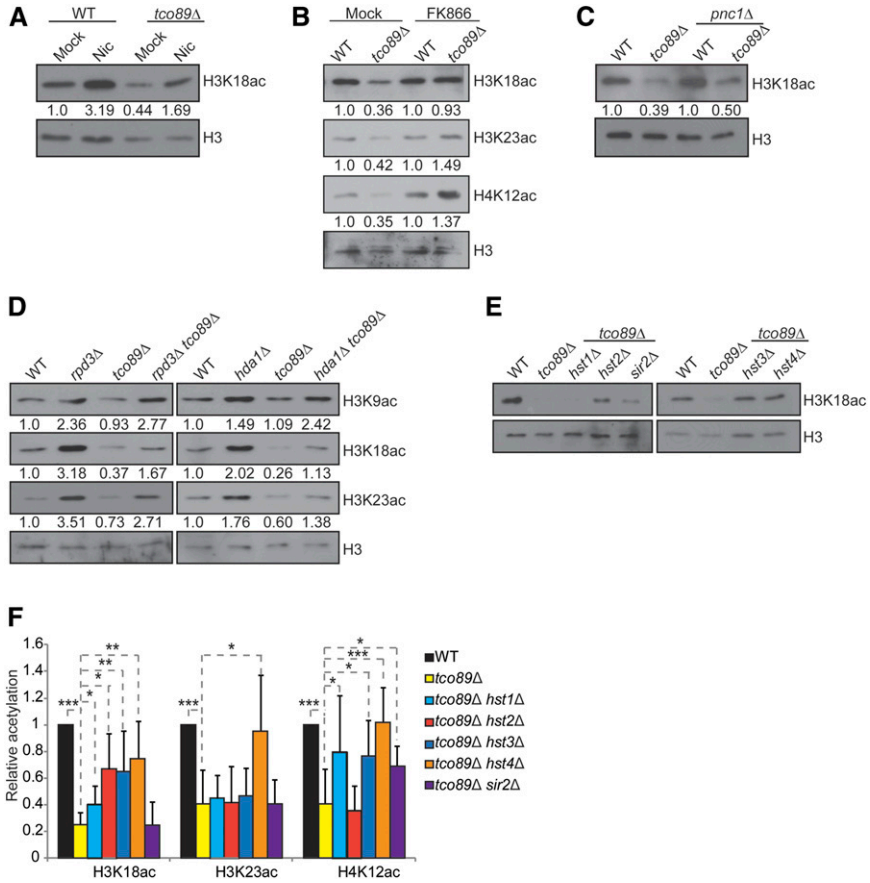

Figure 4 TORC1-responsive histone acetylation is specifically modulated by the sirtuin histone deacetylases in a site-dependent fashion. (A) WT and *tco89Δ* cells were cultured to log phase and then mock or 25 mM nicotinamide treated for 1 hr before harvesting and IB and ImageJ analysis. Relative acetylation values are provided. (B) WT and *tco89Δ* cells were cultured to log phase and mock treated or treated with 500 nM FK866 for 45 min before preparing extracts and analyzing as in A. (C) WT, *tco89Δ*, *pnc1Δ*, *and tco89Δ pnc1Δ* cells were cultured to log phase and whole-cell extracts were analyzed by IB and ImageJ with the indicated antibodies. (D) WT, *rpd3Δ*, *hda1Δ*, *tco89Δ*, *tco89Δ rpd3Δ*, and *tco89Δ hda1Δ* cells were cultured and analyzed as in C. For data presented in A–D, blots and acetylation values (normalized to H3, WT set to 1) are representative of at least three independent replicates. (E) Histone acetylation IB analysis of WT, *tco89Δ*, or *tco89Δ* combined with the indicated sirtuin deletions. (F) Quantification of E. Data in F are the average and SD of four or more independent experiments with significance determined by Student's *t*-test. * $P < 0.05$; ** $P < 0.01$; *** $P < 0.001$.

redundancy may exist between these PP6 regulatory subunits in relation to Hst4 regulation. We then confirmed this Sit4-dependent, TORC1-responsive effect on Hst4 levels was not due to transcriptional or post-transcriptional changes in *HST4* messenger RNA (mRNA) expression by analyzing *HST4*, as well as *HST3* and *SIR2* gene expression by qPCR. Expression of *HST3 and HST4* was not increased in the *tco89Δ* background (Figure 5C), and while we do detect a minor, but statistically significant decrease in *SIR2* mRNA expression in *tco89Δ* relative to WT, its significance is currently unclear.

Hst3 protein degradation has been previously shown to be cell-cycle regulated through Cdk1-dependent phosphorylation and subsequent SCF^{Cdc4}-dependent ubiquitination, leading to its proteasome-mediated degradation (Delgoshaie *et al.* 2014; Edenberg *et al.* 2014). Whether any phosphatase opposes this Cdk1-dependent phosphorylation remains unknown. Hst4 was also identified as a candidate SCF^{Cdc4} substrate, although control of its turnover has not been examined in detail (Mark *et al.* 2014). We wondered whether TORC1-dependent regulation of Hst4 protein expression occurs through altered protein stability. WT and *tco89Δ* strains expressing Hst4-9xMyc were cultured to log phase and then treated with 50 μg/ml CHX to inhibit protein synthesis. As a comparison, we performed an identical experiment with Hst3-9xMyc-expressing cells. Intriguingly, we found that while Hst4 turnover was reduced in *tco89Δ* compared to WT, Hst3 degradation was accelerated in the TORC1 mutant (Figure 5, D and E). In addition we show that in a *tco89Δ sit4Δ* Hst4-9xMyc strain, which previously restored WT levels of Hst4 expression compared to a *tco89Δ* alone (Figure 5B), the rate of Hst4 turnover strongly resembles that detected in WT cells (Figure 5D). Together, these data demonstrate that TORC1 signaling via the Sit4 phosphatase complex regulates the proteolytic decay of the sirtuins Hst4 and Hst3 in an inverse fashion, such that TORC1 promotes Hst4 turnover while it stabilizes Hst3.

Reduced TORC1 signaling and subsequent Sit4 activation promotes Hst4 nuclear accumulation, which precedes the increase in Hst4 protein levels

A subset of metazoan sirtuins have been shown to actively shuttle between the nucleus and the cytoplasm as a function of cell-cycle progression or in response to cellular stress (Vaquero *et al.* 2006; Scher *et al.* 2007; Tanno *et al.* 2007; Hisahara *et al.* 2008). Hst4, which has been proposed to be the yeast SIRT3 ortholog, is normally distributed between the cytoplasm and nucleus. Upon biotin starvation, however, Hst4 accumulates at mitochondria to facilitate mitochondrial protein deacetylation (Madsen *et al.* 2015). As mentioned previously, the best-characterized role that TORC1 suppression, and consequent Sit4 activation, has is to induce nuclear localization of transcription factors controlling the NCR pathway (Cooper 2002). We therefore considered the possibility that reduced TORC1 signaling might also stabilize Hst4 by

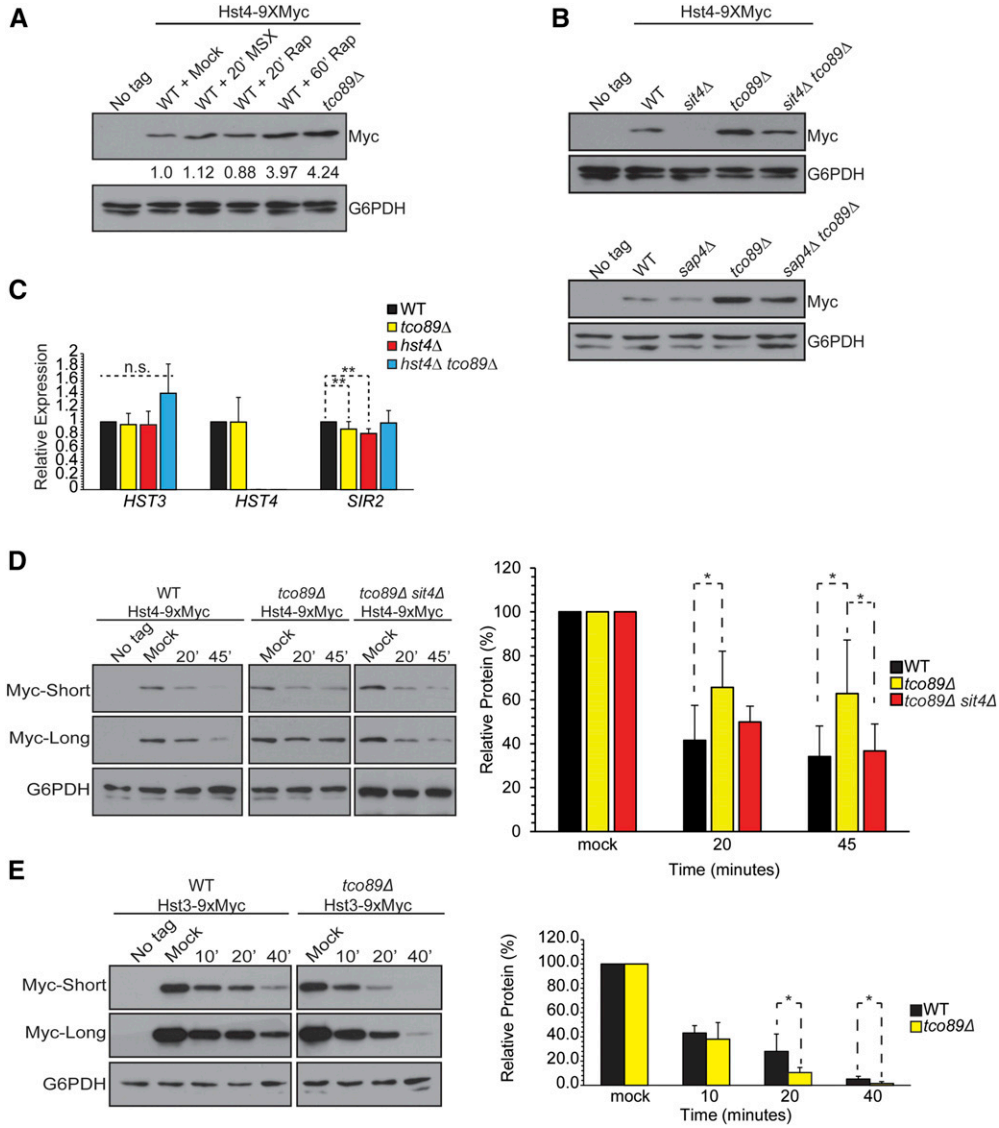

Figure 5 Sit4 activation due to TORC1 inhibition promotes increased Hst4 protein stability. (A) No tag, WT Hst4-9xMyc and *tco89Δ* Hst4-9xMyc were cultured to log phase and WT-tagged cells were then mock treated or treated with 2 mM MSX (20 min) or 300 nM rapamycin (20 min, 60 min) before harvesting. Extracts were prepared and analyzed by IB as indicated. ImageJ analysis was conducted to determine Hst4 levels relative to G6PDH and the average values are provided. Blots and ImageJ data are representative of at least three independent experiments. (B) No tag, WT Hst4-9xMyc, *sit4Δ* Hst4-9xMyc, *sap4Δ* Hst4-9xMyc, *tco89Δ* Hst4-9xMyc, *sit4Δ tco89Δ* Hst4-9xMyc, and *sap4Δ tco89Δ* Hst4-9xMyc cells were cultured and analyzed as in A. (C) WT, *tco89Δ*, *hst4Δ*, and *tco89Δ hst4Δ* cells were cultured to log phase, total RNA was extracted, cDNA was synthesized, and qPCR performed with the indicated primer sets. Data are the average and SD of four independent experiments, and significance was determined by Student's *t*-test. * $P < 0.05$; ** $P < 0.01$; *** $P < 0.001$. (D) Strains from B were cultured to log phase and treated with 50 μg/ml CHX. Samples were taken at T_0 prior to CHX addition and then again at T_{20} and T_{45}. Short and long exposures of the α-Myc blot are shown for clarity, and quantification of the data is provided. Data are average and SD of four independent biological replicates and significance was determined as in C. (E) As in D, except Hst3 stability is being measured. Time points differ from D as indicated.

altering its cellular distribution. To test this, WT and *tco89Δ* cells expressing either Hst4-9xMyc or the other tagged sirtuins, were cultured to log phase before performing α-Myc immunostaining and quantitative confocal microscopy analysis. Random fields of cells were captured and the amount of nuclear sirtuin was manually quantified as described in *Materials and Methods*. Representative images for Hst4 are shown in Figure 6A and for all five sirtuins in Figure S4. Intriguingly, *tco89Δ* enhanced the Hst4 nuclear pool, even after accounting for the increase in Hst4 protein levels (Figure 6, A and B). A minor increase in Sir2 nuclear accumulation was also detected but none of the other sirtuins, including Hst3, exhibited a significant change in localization (Figure 6B and Figure S4). To specifically address whether the increase in Hst4 nuclear localization occurred before or after Hst4 protein levels were increased, we repeated the WT and *tco89Δ* Hst4-9xMyc immunostaining experiment, this time including an additional WT sample treated with 200 nM rapamycin for 20 min. We detected maximal Hst4 relocalization within 20 min after rapamycin addition, which was approximately equivalent to the amount of nuclear-localized Hst4 observed in *tco89Δ* (Figure 6C and Figure S4). This relocalization is far earlier than the observed increase in protein levels (Figure 5A), and it correlates with the decrease in histone acetylation (Figure S1B). Finally, we asked whether this relocalization was dependent on Sit4 activation downstream of TORC1 inhibition, since Sit4 regulates Hst4 protein levels (Figure 5, B and D). Strikingly, we found that in a *tco89Δ sit4Δ* Hst4-9xMyc strain, the cytoplasmic population of Hst4 is restored to near WT levels (Figure 6, A and C), supporting the hypothesis that decreased TORC1 signaling triggers Sit4/PP6 activation, which

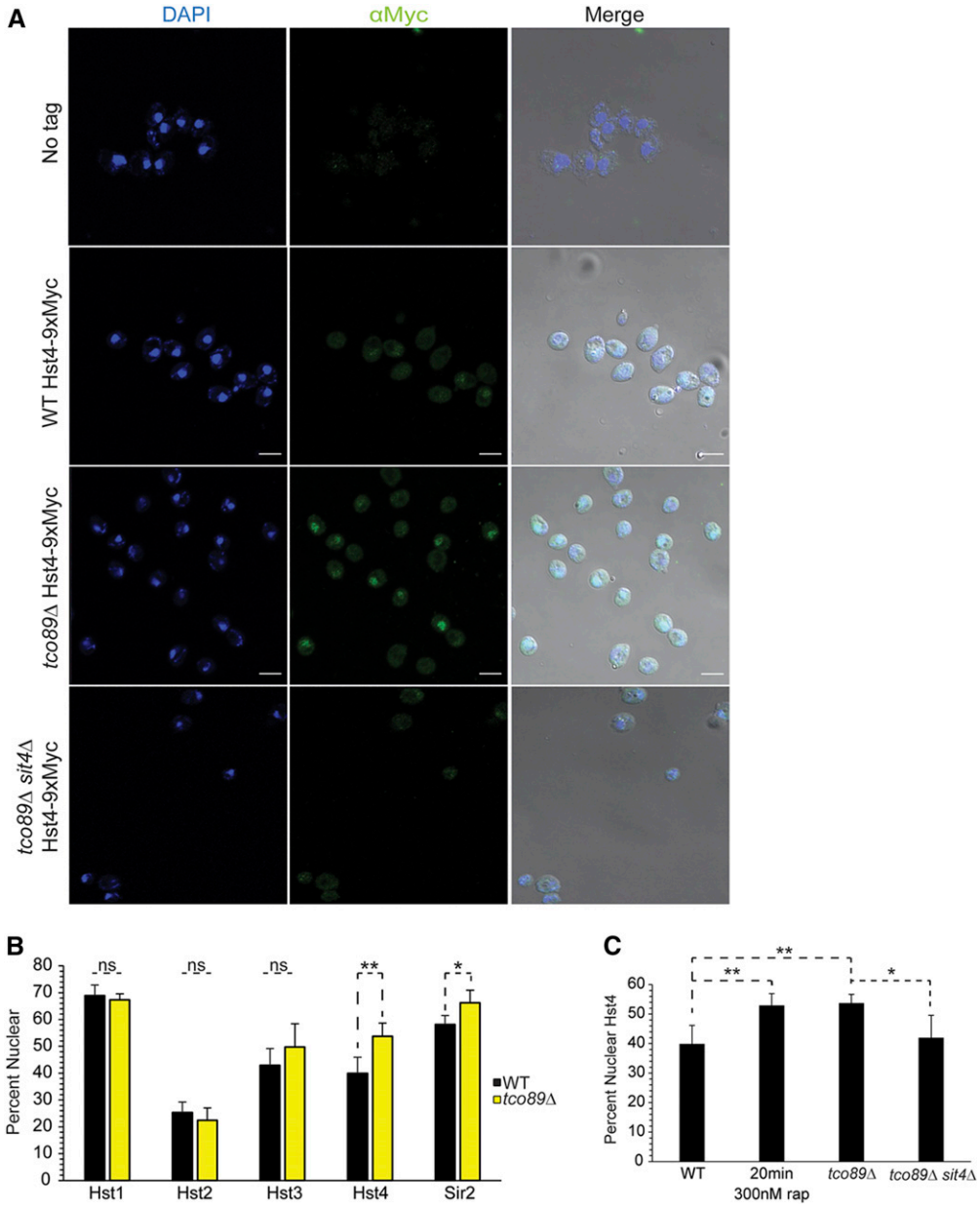

Figure 6 Hst4 nuclear relocalization occurs rapidly as a consequence of TORC1 inhibition and Sit4 activation, which precedes the increase in Hst4 stability. (A) Representative confocal microscopy of WT, *tco89Δ* Hst4-9xMyc, and *tco89Δ sit4Δ* Hst4-9xMyc expressing cells. Cells without a Myc tag (no tag) are included as an indicator of background fluorescence. (B) Quantification of sirtuin microscopy images, including those shown in A and Figure S4, was performed as described in *Materials and Methods*. Data represented are the average and SD of four independent experiments and significance was determined by Student's *t*-test. * $P < 0.05$; ** $P < 0.01$. (C) As in B, except WT Hst4-9xMyc cells were mock or rapamycin treated (300 nM, 20 min) prior to imaging. *tco89Δ* Hst4-9xMyc and *tco89Δ sit4Δ* Hst4-9xMyc cells are included for comparison.

promotes Hst4 nuclear localization and stabilization to mediate site-specific histone deacetylation.

Hst4-regulated histone acetylation controls a subset of TORC1-dependent biological functions

TORC1 was identified previously to regulate acetylation of the RP genes through the recruitment of the Esa1 acetyltransferase (Rohde and Cardenas 2003). The initial Tco89 characterization conducted by Reinke *et al.* (2004) determined *tco89Δ* has no effect on RP gene transcription. Given the observed acetylation defects in *tco89Δ*, we chose to independently determine whether reduced TORC1 signaling may alter RP gene expression through an Hst4-dependent mechanism. Similar to the findings reported by Reinke *et al.* (2004), we found that although TORC1 activity is reduced in *tco89Δ* (Figure S1A), no significant decrease in *tco89Δ* RP gene expression occurred (Figure 7A). Additionally, the *hst4Δ* had no effect on RP gene expression, and while *tco89Δ hst4Δ* modestly reduced expression of *RPL23B*, *tco89Δ hst4Δ* did not affect the expression of the other RP genes (Figure 7A). These data indicate that the residual TORC1 activity retained in *tco89Δ* is sufficient to maintain normal RP gene expression and that Hst4 does not significantly contribute to their regulation.

Previous studies demonstrated that exposure to nutrient starvation or rapamycin treatment causes *tco89Δ* cells to exit the cell cycle and enter into an irreversible, G_0-like growth arrested state (Binda *et al.* 2009). We next asked whether restoration of TORC1-mediated histone acetylation could rescue the sensitivity of *tco89Δ* mutants to multiple conditions that impair TORC1 signaling (Hosiner *et al.* 2009; Kapitzky *et al.* 2010). We found this effect was reversed in

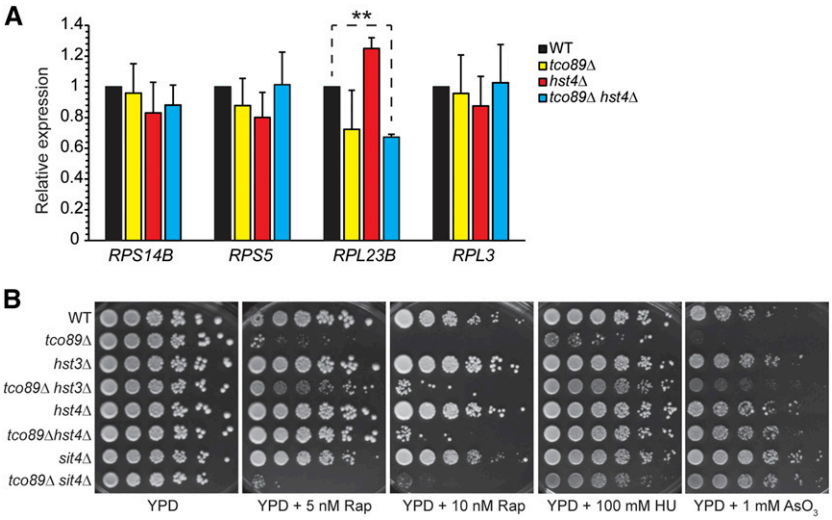

Figure 7 TORC1-mediated histone acetylation does not impact RP gene transcription but is involved in the DNA-damage response and cell-cycle progression. (A) WT, *tco89Δ*, *hst4Δ*, and *tco89Δ hst4Δ* cells were cultured to log phase, total RNA was extracted, cDNA was synthesized, and qPCR performed with the indicated primer sets. Data are the average and SD of three independent experiments and significance was determined by Student's *t*-test. (B) WT, *tco89Δ*, *hst3Δ*, *tco89Δ hst3Δ*, *hst4Δ*, *tco89Δ hst4Δ*, *sit4Δ*, and *tco89Δ sit4Δ* were cultured overnight to saturation. Equal numbers of cells were serially diluted fivefold and spotted onto YPD, YPD 5 nM rapamycin, YPD 10 nM rapamycin, YPD 100 mM hydroxyurea (HU), and YPD 1 mM arsenic oxide (AsO_3). Images were taken 4 days after spotting.

a *tco89Δ hst4Δ* mutant, and to a lesser extent in *tco89Δ hst3Δ*, under low (5 nM) rapamycin concentrations (Figure 7B). Surprisingly, at slightly higher (10 nM) rapamycin concentrations, neither double mutant grew significantly (Figure 7B). Intriguingly, the *tco89Δ sit4Δ* failed to restore growth in the presence of even the low rapamycin concentration; however, combining *tco89Δ* with either *hst3Δ*, *hst4Δ*, or *sit4Δ* completely restored growth on both hydroxyurea and arsenic (Figure 7B). These results demonstrate that sirtuins are important for maintaining the G_0-like growth-arrested state that TORC1 mutants exhibit when exposed to environmental stressors that inhibit TORC1 activity. However, while Sit4 loss can rescue this growth arrest in the presence of some TORC1 inhibitors, it appears to have functions independent of its link to sirtuins that are required for TORC1 impaired cells to escape the growth arrest induced specifically by rapamycin.

Discussion

The epigenome of eukaryotic cells is responsive to environmental stimuli, including changes in nutrient availability. Previous studies have shown that TORC1 signaling affects epigenetic processes, including mediating Esa1 recruitment to RP genes to acetylate histone H4, as well as regulating global H3K56ac (Rohde and Cardenas 2003; Chen *et al.* 2012). In this report, we significantly expand our understanding of the mechanistic link between TORC1 signaling and its downstream effects on site-specific histone acetylation modifications. We demonstrate for the first time that in logarithmically growing cells, TORC1 inhibition results in a rapid, direct, and selective deacetylation of H3K18, H3K23, and H4K12 on the histone H3/H4 N termini. To date, studies examining TORC1-regulated acetylation have used the TORC1 inhibitor rapamycin to examine the functional consequences TORC1 activity has on chromatin (Rohde and Cardenas 2003; Ha and Huh 2011; Chen *et al.* 2012). And while we also utilized rapamycin for this purpose, we extended our analyses to include other methods to suppress TORC1, including subunit deletion (*tco89Δ*) and a pharmacological inhibitor of nitrogen metabolism (MSX) (Crespo *et al.* 2002). We provide clear evidence that either of these additional conditions are sufficient to decrease site-specific histone H3/H4 acetylation, thus implicating nitrogen-dependent TORC1 activation as a significant regulator of histone acetylation.

Previous studies demonstrated that stationary phase cells exhibit reduced histone acetylation at many of the same residues identified above (Friis *et al.* 2009). These acetylation states were rescued by glucose refeeding, suggesting that carbon metabolism is a significant regulator of these histone modifications. However, we find that culturing WT and *tco89Δ* cells in media containing either a preferred, fermentable (glucose) carbon or a nonpreferred, nonfermentable (glycerol) carbon source, resulted in no change to the spectrum of observed histone acetylation defects. Our data argue against the possibility that crosstalk between carbon metabolism and TORC1 regulation, as was previously suggested, is ultimately responsible for the chromatin effects we observe (Schmelzle *et al.* 2004; Dechant *et al.* 2014). Instead, our findings suggest that in actively growing cells, nitrogen signaling through TORC1 is the predominant regulator of these specific histone acetylation states. As a consequence, the vacuole likely serves a vital link in the transmission of environmental nutrient sufficiency to the epigenetic regulatory apparatus via TORC1 activation. Indeed, a previous genetic screen of the systematic yeast deletion collection identified several vacuole mutants, including many V-ATPase mutants, to be necessary for maintenance of global histone acetylation (Peng *et al.* 2008).

Our study also provides a more detailed mechanistic understanding of our previous work, which identified a functional relationship between TORC1, sirtuins, and the regulation of H3K56ac. We demonstrate by direct pharmacological inhibition, cofactor depletion, and individual sirtuin deletion that TORC1 signaling specifically opposes histone deacetylation mediated by several sirtuin family members. Importantly,

Hst4 was the only sirtuin that, when deleted in a *tco89Δ* background, restored acetylation across all of the known TORC1-regulated residues. This suggests that while TORC1 may have a general role in opposing sirtuin activity, Hst4 is likely to be one of the predominant sirtuins whose function is negatively affected by signaling through this pathway. The intimate link between TORC1 and the sirtuins is interesting, considering that both are responsive to cellular energetics, albeit inversely. This relationship appears to be conserved at some level across all eukaryotes (Ha and Huh 2011; Chen *et al.* 2012; Csibi *et al.* 2013; Jack *et al.* 2015). Together, our data support a model whereby TORC1 and sirtuin activity are regulated in an opposing manner to coordinate both nitrogen and energy metabolism with epigenetic control to facilitate productive cell growth and proliferation.

The presented findings also implicate TORC1-dependent suppression of the Tap42-associated Sit4 containing PP6 phosphatase complex in the regulation of histone acetylation. We demonstrate that these effects are independent of changes in *HST4* gene expression, and that Sit4-regulated histone acetylation suppression is separable from Sit4-dependent activation of the NCR pathway. Instead, we provide support for a mechanism in which Sit4 activation promotes both a rapid cytoplasmic-to-nuclear redistribution of Hst4, and an eventual increase in Hst4 protein levels due to reduced protein turnover. Considering that maximal Hst4 relocalization occurs within 20 min post-TORC1 inhibition, but Hst4 protein does not accumulate significantly until ~40 min later, Hst4 movement to the nucleus may function to shield a fraction of the enzyme from proteolytic turnover. These effects on Hst4 are unique, as identical experiments with a highly similar sirtuin, Hst3, revealed that lower TORC1 activity does not affect Hst3 nuclear localization but does decrease Hst3 protein stability. How TORC1-dependent suppression of the Sit4 phosphatase causes these opposing effects on Hst3 and Hst4 stability is the subject of ongoing investigation. A distinct possibility is that changes in nutrient sufficiency modify TORC1-regulated Sit4 activity to affect Hst3 and Hst4 phosphorylation status and regulate their SCF^{Cdc4}-dependent turnover. Such a regulatory mechanism might better coordinate the cellular growth response with cell division timing, as all of these factors are also intimately connected to cell-cycle regulation.

Histone acetylation regulates gene expression, in part, by disrupting histone–DNA contacts to promote chromatin decondensation, as well as by serving as docking sites for bromodomain- or YEATS-domain-containing regulatory factors (Sanchez *et al.* 2014; Shanle *et al.* 2015). While TORC1 signaling is known to regulate the transcription of a large number of genes involved in cell growth and proliferation, the functional contributions our newly characterized TORC1-regulated histone acetylation states have in relation to these processes are currently unclear. In agreement with a previous report (Reinke *et al.* 2004), we find that in the *tco89Δ* TORC1 mutant, RP gene expression is largely unaffected. We believe this demonstrates that there is sufficient residual TORC1 activity present in these mutants to maintain basal Sch9 activation and RP gene expression. However, TORC1 transcriptional regulation extends beyond just RP genes, so it is likely that other genes will be preferentially sensitive to the reduced histone acetylation we have detected. Identifying which acetyl lysine binding proteins are affected by altered TORC1 signaling will be critical to completely define how TORC1-dependent histone acetylation contributes to transcriptional programs controlling growth and proliferation.

Cells deficient in TORC1, such as *tco89Δ* mutants, are acutely sensitive to environmental exposures that suppress TORC1 signaling, including rapamycin, DNA replication inhibitors, metals, and a variety of other stress-inducing agents. And while these compounds are often grouped together as having a generalized inhibitory effect on TORC1, the downstream cellular responses they elicit can vary substantially (Tate and Cooper 2013; Hughes Hallett *et al.* 2014). We demonstrate that the TORC1–PP6–sirtuin pathway outlined above is functionally relevant for a subset of TORC1-regulated biological processes, as either *hst3Δ* or *hst4Δ* can suppress *tco89Δ* sensitivity to arsenic, hydroxyurea, and low concentrations of rapamycin. We believe that these sirtuins may contribute to enforcing the cell-cycle exit that occurs in *tco89Δ* exposed to TORC1 suppressive conditions, in part through their role in chromatin deacetylation. Loss of either sirtuin may facilitate cell-cycle reentry following TORC1 inhibition by maintaining a more basally hyperacetylated, transcriptionally permissive chromatin state, thus allowing for more facile induction of genes necessary to escape the arrested state. The recent identification of a glucose-regulated histone acetylation pathway necessary for transcription of the *CLN3* cyclin, and subsequent entry into the cell cycle, provides support for this concept (Shi and Tu 2013).

Furthermore, we demonstrate that while *sit4Δ* also rescues the sensitivity of *tco89Δ* to both hydroxyurea and arsenic, it fails to promote growth on rapamycin. These results suggest the possibility that Sit4 has sirtuin-independent roles in regulating cell growth control that are necessary for TORC1-deficient cells to escape the rapamycin-induced growth arrest (Sutton *et al.* 1991; Fernandez-Sarabia *et al.* 1992). There is a precedent for Tap42-associated phosphatases regulating such dynamics as it was previously shown that the nitrogen-responsive Rim15-dependent phosphorylation of PP2A phosphatase plays a critical role in cell-cycle entry, as well as exit from quiescence (Bontron *et al.* 2013). Another candidate explanation is that Sit4 association with distinct Sap regulatory factors may have context-specific effects. In support of this, a previous report determined that the function Sit4 has in response to TORC1 suppression depends on the identity of the associated Sap regulator (Rohde *et al.* 2004). Unraveling these differences, and their specific role in sirtuin regulation, will be the subject of future studies.

Overall, our data define a mechanism by which nitrogen signaling through TORC1 activation controls specific epigenetic modifications that are important for TORC1-regulated cell growth and proliferation. Because these pathways are conserved in mammals, we consider it highly likely that deregulation of nitrogen metabolism and aberrant mTORC1 activation, which occurs in many cancers, might alter the epigenome through similar mechanisms to promote disease pathogenesis.

Acknowledgments

We thank Daniel Klionsky for the Tap42 yeast strains, Mary Miller for assistance with tetrad dissection, and Brian Strahl for critical comments regarding manuscript preparation. Research in the Laribee laboratory is supported by National Institutes of Health grant 1R01-GM107040-01 awarded to R.N.L.

Literature Cited

Beck, T., and M. N. Hall, 1999 The TOR signalling pathway controls nuclear localization of nutrient-regulated transcription factors. Nature 402: 689–692.

Binda, M., M. P. Peli-Gulli, G. Bonfils, N. Panchaud, J. Urban *et al.*, 2009 The Vam6 GEF controls TORC1 by activating the EGO complex. Mol. Cell 35: 563–573.

Bontron, S., M. Jaquenoud, S. Vaga, N. Talarek, B. Bodenmiller *et al.*, 2013 Yeast endosulfines control entry into quiescence and chronological life span by inhibiting protein phosphatase 2A. Cell Reports 3: 16–22.

Cardenas, M. E., N. S. Cutler, M. C. Lorenz, C. J. Di Como, and J. Heitman, 1999 The TOR signaling cascade regulates gene expression in response to nutrients. Genes Dev. 13: 3271–3279.

Chen, H., M. Fan, L. M. Pfeffer, and R. N. Laribee, 2012 The histone H3 lysine 56 acetylation pathway is regulated by target of rapamycin (TOR) signaling and functions directly in ribosomal RNA biogenesis. Nucleic Acids Res. 40: 6534–6546.

Cooper, T. G., 2002 Transmitting the signal of excess nitrogen in Saccharomyces cerevisiae from the Tor proteins to the GATA factors: connecting the dots. FEMS Microbiol. Rev. 26: 223–238.

Crespo, J. L., T. Powers, B. Fowler, and M. N. Hall, 2002 The TOR-controlled transcription activators GLN3, RTG1, and RTG3 are regulated in response to intracellular levels of glutamine. Proc. Natl. Acad. Sci. USA 99: 6784–6789.

Csibi, A., S. M. Fendt, C. Li, G. Poulogiannis, A. Y. Choo *et al.*, 2013 The mTORC1 pathway stimulates glutamine metabolism and cell proliferation by repressing SIRT4. Cell 153: 840–854.

Dechant, R., S. Saad, A. J. Ibanez, and M. Peter, 2014 Cytosolic pH regulates cell growth through distinct GTPases, Arf1 and Gtr1, to promote Ras/PKA and TORC1 activity. Mol. Cell 55: 409–421.

Delgoshaie, N., X. Tang, E. D. Kanshin, E. C. Williams, A. D. Rudner *et al.*, 2014 Regulation of the histone deacetylase Hst3 by cyclin-dependent kinases and the ubiquitin ligase SCFCdc4. J. Biol. Chem. 289: 13186–13196.

Di Como, C. J., and K. T. Arndt, 1996 Nutrients, via the Tor proteins, stimulate the association of Tap42 with type 2A phosphatases. Genes Dev. 10: 1904–1916.

Edenberg, E. R., A. A. Vashisht, B. R. Topacio, J. A. Wohlschlegel, and D. P. Toczyski, 2014 Hst3 is turned over by a replication stress-responsive SCF(Cdc4) phospho-degron. Proc. Natl. Acad. Sci. USA 111: 5962–5967.

Fernandez-Sarabia, M. J., A. Sutton, T. Zhong, and K. T. Arndt, 1992 SIT4 protein phosphatase is required for the normal accumulation of SWI4, CLN1, CLN2, and HCS26 RNAs during late G1. Genes Dev. 6: 2417–2428.

Friis, R. M., B. P. Wu, S. N. Reinke, D. J. Hockman, B. D. Sykes *et al.*, 2009 A glycolytic burst drives glucose induction of global histone acetylation by picNuA4 and SAGA. Nucleic Acids Res. 37: 3969–3980.

Ghosh, H. S., M. McBurney, and P. D. Robbins, 2010 SIRT1 negatively regulates the mammalian target of rapamycin. PLoS One 5: e9199.

Gonzalez, A., M. Shimobayashi, T. Eisenberg, D. A. Merle, T. Pendl *et al.*, 2015 TORC1 promotes phosphorylation of ribosomal protein S6 via the AGC kinase Ypk3 in Saccharomyces cerevisiae. PLoS One 10: e0120250.

Guo, W., L. Qian, J. Zhang, W. Zhang, A. Morrison *et al.*, 2011 Sirt1 overexpression in neurons promotes neurite outgrowth and cell survival through inhibition of the mTOR signaling. J. Neurosci. Res. 89: 1723–1736.

Ha, C. W., and W. K. Huh, 2011 Rapamycin increases rDNA stability by enhancing association of Sir2 with rDNA in Saccharomyces cerevisiae. Nucleic Acids Res. 39: 1336–1350.

Hardwick, J. S., F. G. Kuruvilla, J. K. Tong, A. F. Shamji, and S. L. Schreiber, 1999 Rapamycin-modulated transcription defines the subset of nutrient-sensitive signaling pathways directly controlled by the Tor proteins. Proc. Natl. Acad. Sci. USA 96: 14866–14870.

Hasmann, M., and I. Schemainda, 2003 FK866, a highly specific noncompetitive inhibitor of nicotinamide phosphoribosyltransferase, represents a novel mechanism for induction of tumor cell apoptosis. Cancer Res. 63: 7436–7442.

Hisahara, S., S. Chiba, H. Matsumoto, M. Tanno, H. Yagi *et al.*, 2008 Histone deacetylase SIRT1 modulates neuronal differentiation by its nuclear translocation. Proc. Natl. Acad. Sci. USA 105: 15599–15604.

Hombauer, H., D. Weismann, I. Mudrak, C. Stanzel, T. Fellner *et al.*, 2007 Generation of active protein phosphatase 2A is coupled to holoenzyme assembly. PLoS Biol. 5: e155.

Hosiner, D., H. Lempiainen, W. Reiter, J. Urban, R. Loewith *et al.*, 2009 Arsenic toxicity to Saccharomyces cerevisiae is a consequence of inhibition of the TORC1 kinase combined with a chronic stress response. Mol. Biol. Cell 20: 1048–1057.

Huber, A., B. Bodenmiller, A. Uotila, M. Stahl, S. Wanka *et al.*, 2009 Characterization of the rapamycin-sensitive phosphoproteome reveals that Sch9 is a central coordinator of protein synthesis. Genes Dev. 23: 1929–1943.

Huber, A., S. L. French, H. Tekotte, S. Yerlikaya, M. Stahl *et al.*, 2011 Sch9 regulates ribosome biogenesis via Stb3, Dot6 and Tod6 and the histone deacetylase complex RPD3L. EMBO J. 30: 3052–3064.

Hughes Hallett, J. E., X. Luo, and A. P. Capaldi, 2014 State transitions in the TORC1 signaling pathway and information processing in Saccharomyces cerevisiae. Genetics 198: 773–786.

Imai, S., and L. Guarente, 2014 NAD+ and sirtuins in aging and disease. Trends Cell Biol. 24: 464–471.

Jack, C. V., C. Cruz, R. M. Hull, M. A. Keller, M. Ralser *et al.*, 2015 Regulation of ribosomal DNA amplification by the TOR pathway. Proc. Natl. Acad. Sci. USA 112: 9674–9679.

Janke, C., M. M. Magiera, N. Rathfelder, C. Taxis, S. Reber *et al.*, 2004 A versatile toolbox for PCR-based tagging of yeast genes: new fluorescent proteins, more markers and promoter substitution cassettes. Yeast 21: 947–962.

Jiang, Y., and J. R. Broach, 1999 Tor proteins and protein phosphatase 2A reciprocally regulate Tap42 in controlling cell growth in yeast. EMBO J. 18: 2782–2792.

Kapitzky, L., P. Beltrao, T. J. Berens, N. Gassner, C. Zhou *et al.*, 2010 Cross-species chemogenomic profiling reveals evolutionarily conserved drug mode of action. Mol. Syst. Biol. 6: 451.

Kuruvilla, F. G., A. F. Shamji, and S. L. Schreiber, 2001 Carbon- and nitrogen-quality signaling to translation are mediated by distinct GATA-type transcription factors. Proc. Natl. Acad. Sci. USA 98: 7283–7288.

Laplante, M., and D. M. Sabatini, 2012 mTOR signaling in growth control and disease. Cell 149: 274–293.

Laribee, R. N., A. Hosni-Ahmed, J. J. Workman, and H. Chen, 2015 Ccr4-not regulates RNA polymerase I transcription and couples nutrient signaling to the control of ribosomal RNA biogenesis. PLoS Genet. 11: e1005113.

Loewith, R., and M. N. Hall, 2011 Target of rapamycin (TOR) in nutrient signaling and growth control. Genetics 189: 1177–1201.

Loewith, R., E. Jacinto, S. Wullschleger, A. Lorberg, J. L. Crespo *et al.*, 2002 Two TOR complexes, only one of which is rapamycin sensitive, have distinct roles in cell growth control. Mol. Cell 10: 457–468.

Lu, C., and C. B. Thompson, 2012 Metabolic regulation of epigenetics. Cell Metab. 16: 9–17.

Luke, M. M., F. Della Seta, C. J. Di Como, H. Sugimoto, R. Kobayashi *et al.*, 1996 The SAP, a new family of proteins, associate and function positively with the SIT4 phosphatase. Mol. Cell. Biol. 16: 2744–2755.

Madsen, C. T., K. B. Sylvestersen, C. Young, S. C. Larsen, J. W. Poulsen *et al.*, 2015 Biotin starvation causes mitochondrial protein hyperacetylation and partial rescue by the SIRT3-like deacetylase Hst4p. Nat. Commun. 6: 7726.

Mark, K. G., M. Simonetta, A. Maiolica, C. A. Seller, and D. P. Toczyski, 2014 Ubiquitin ligase trapping identifies an SCF (Saf1) pathway targeting unprocessed vacuolar/lysosomal proteins. Mol. Cell 53: 148–161.

Medvedik, O., D. W. Lamming, K. D. Kim, and D. A. Sinclair, 2007 MSN2 and MSN4 link calorie restriction and TOR to sirtuin-mediated lifespan extension in Saccharomyces cerevisiae. PLoS Biol. 5: e261.

Mumberg, D., R. Muller, and M. Funk, 1995 Yeast vectors for the controlled expression of heterologous proteins in different genetic backgrounds. Gene 156: 119–122.

Peng, W., C. Togawa, K. Zhang, and S. K. Kurdistani, 2008 Regulators of cellular levels of histone acetylation in Saccharomyces cerevisiae. Genetics 179: 277–289.

Ramachandran, V., and P. K. Herman, 2011 Antagonistic interactions between the cAMP-dependent protein kinase and Tor signaling pathways modulate cell growth in Saccharomyces cerevisiae. Genetics 187: 441–454.

Reinke, A., S. Anderson, J. M. McCaffery, J. Yates, 3rd, S. Aronova *et al.*, 2004 TOR complex 1 includes a novel component, Tco89p (YPL180w), and cooperates with Ssd1p to maintain cellular integrity in Saccharomyces cerevisiae. J. Biol. Chem. 279: 14752–14762.

Rohde, J. R., and M. E. Cardenas, 2003 The tor pathway regulates gene expression by linking nutrient sensing to histone acetylation. Mol. Cell. Biol. 23: 629–635.

Rohde, J. R., S. Campbell, S. A. Zurita-Martinez, N. S. Cutler, M. Ashe *et al.*, 2004 TOR controls transcriptional and translational programs via Sap-Sit4 protein phosphatase signaling effectors. Mol. Cell. Biol. 24: 8332–8341.

Rundlett, S. E., A. A. Carmen, R. Kobayashi, S. Bavykin, B. M. Turner *et al.*, 1996 HDA1 and RPD3 are members of distinct yeast histone deacetylase complexes that regulate silencing and transcription. Proc. Natl. Acad. Sci. USA 93: 14503–14508.

Sanchez, R., J. Meslamani, and M. M. Zhou, 2014 The bromodomain: from epigenome reader to druggable target. Biochim. Biophys. Acta 1839: 676–685.

Scher, M. B., A. Vaquero, and D. Reinberg, 2007 SirT3 is a nuclear NAD+-dependent histone deacetylase that translocates to the mitochondria upon cellular stress. Genes Dev. 21: 920–928.

Schmelzle, T., T. Beck, D. E. Martin, and M. N. Hall, 2004 Activation of the RAS/cyclic AMP pathway suppresses a TOR deficiency in yeast. Mol. Cell. Biol. 24: 338–351.

Shanle, E. K., F. H. Andrews, H. Meriesh, S. L. McDaniel, R. Dronamraju *et al.*, 2015 Association of Taf14 with acetylated histone H3 directs gene transcription and the DNA damage response. Genes Dev. 29: 1795–1800.

Shi, L., and B. P. Tu, 2013 Acetyl-CoA induces transcription of the key G1 cyclin CLN3 to promote entry into the cell division cycle in Saccharomyces cerevisiae. Proc. Natl. Acad. Sci. USA 110: 7318–7323.

Soulard, A., A. Cremonesi, S. Moes, F. Schutz, P. Jeno *et al.*, 2010 The rapamycin-sensitive phosphoproteome reveals that TOR controls protein kinase A toward some but not all substrates. Mol. Biol. Cell 21: 3475–3486.

Sutton, A., D. Immanuel, and K. T. Arndt, 1991 The SIT4 protein phosphatase functions in late G1 for progression into S phase. Mol. Cell. Biol. 11: 2133–2148.

Szyf, M., 2015 Nongenetic inheritance and transgenerational epigenetics. Trends Mol. Med. 21: 134–144.

Tanno, M., J. Sakamoto, T. Miura, K. Shimamoto, and Y. Horio, 2007 Nucleocytoplasmic shuttling of the NAD+-dependent histone deacetylase SIRT1. J. Biol. Chem. 282: 6823–6832.

Tate, J. J., and T. G. Cooper, 2013 Five conditions commonly used to down-regulate tor complex 1 generate different physiological situations exhibiting distinct requirements and outcomes. J. Biol. Chem. 288: 27243–27262.

Urban, J., A. Soulard, A. Huber, S. Lippman, D. Mukhopadhyay *et al.*, 2007 Sch9 is a major target of TORC1 in Saccharomyces cerevisiae. Mol. Cell 26: 663–674.

Vaquero, A., M. B. Scher, D. H. Lee, A. Sutton, H. L. Cheng *et al.*, 2006 SirT2 is a histone deacetylase with preference for histone H4 Lys 16 during mitosis. Genes Dev. 20: 1256–1261.

Wei, Y., and X. F. Zheng, 2009 Sch9 partially mediates TORC1 signaling to control ribosomal RNA synthesis. Cell Cycle 8: 4085–4090.

Wierman, M. B., and J. S. Smith, 2014 Yeast sirtuins and the regulation of aging. FEMS Yeast Res. 14: 73–88.

Yan, G., Y. Lai, and Y. Jiang, 2012 The TOR complex 1 is a direct target of Rho1 GTPase. Mol. Cell 45: 743–753.

Yorimitsu, T., C. He, K. Wang, and D. J. Klionsky, 2009 Tap42-associated protein phosphatase type 2A negatively regulates induction of autophagy. Autophagy 5: 616–624.

Communicating editor: M. Hampsey

GENETICS

Supporting Information
www.genetics.org/lookup/suppl/doi:10.1534/genetics.116.188458/-/DC1

Saccharomyces cerevisiae TORC1 Controls Histone Acetylation by Signaling Through the Sit4/PP6 Phosphatase to Regulate Sirtuin Deacetylase Nuclear Accumulation

Jason J. Workman, Hongfeng Chen, and R. Nicholas Laribee

DOI: 10.1534/genetics.116.188458

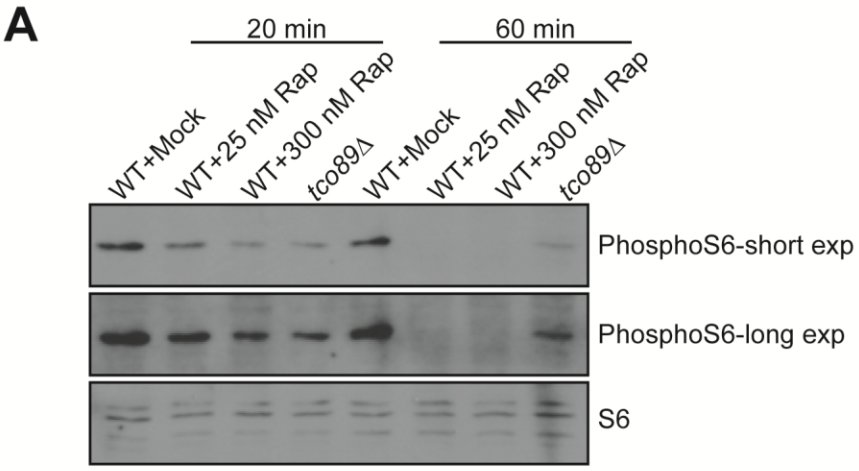
A
20 min
60 min
WT+Mock
WT+25 nM Rap
WT+300 nM Rap
tco89Δ
WT+Mock
WT+25 nM Rap
WT+300 nM Rap
tco89Δ
PhosphoS6-short exp
PhosphoS6-long exp
S6

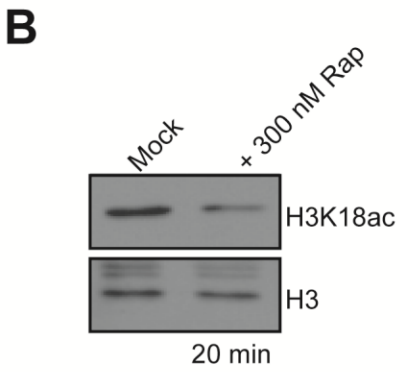
B
Mock
+ 300 nM Rap
H3K18ac
H3
20 min

Figure S1

Figure S1. Optimization of rapamycin treatment conditions. (A) Wild-type (WT) and *tco89Δ* cells were cultured to log phase, and WT cells were then mock treated, or treated with varying rapamycin concentrations (25 nM or 300 nM) for either 20 minutes or 60 minutes. Whole-cell extracts were prepared and analyzed by immunoblot (IB) with the indicated antibodies. Short and long exposures for the phosphoS6 blots are presented for clarity. (B) WT cells were cultured to log phase and then mock treated or treated with 300 nM rapamycin for 20 minutes. Extracts were prepared and analyzed as in (A).

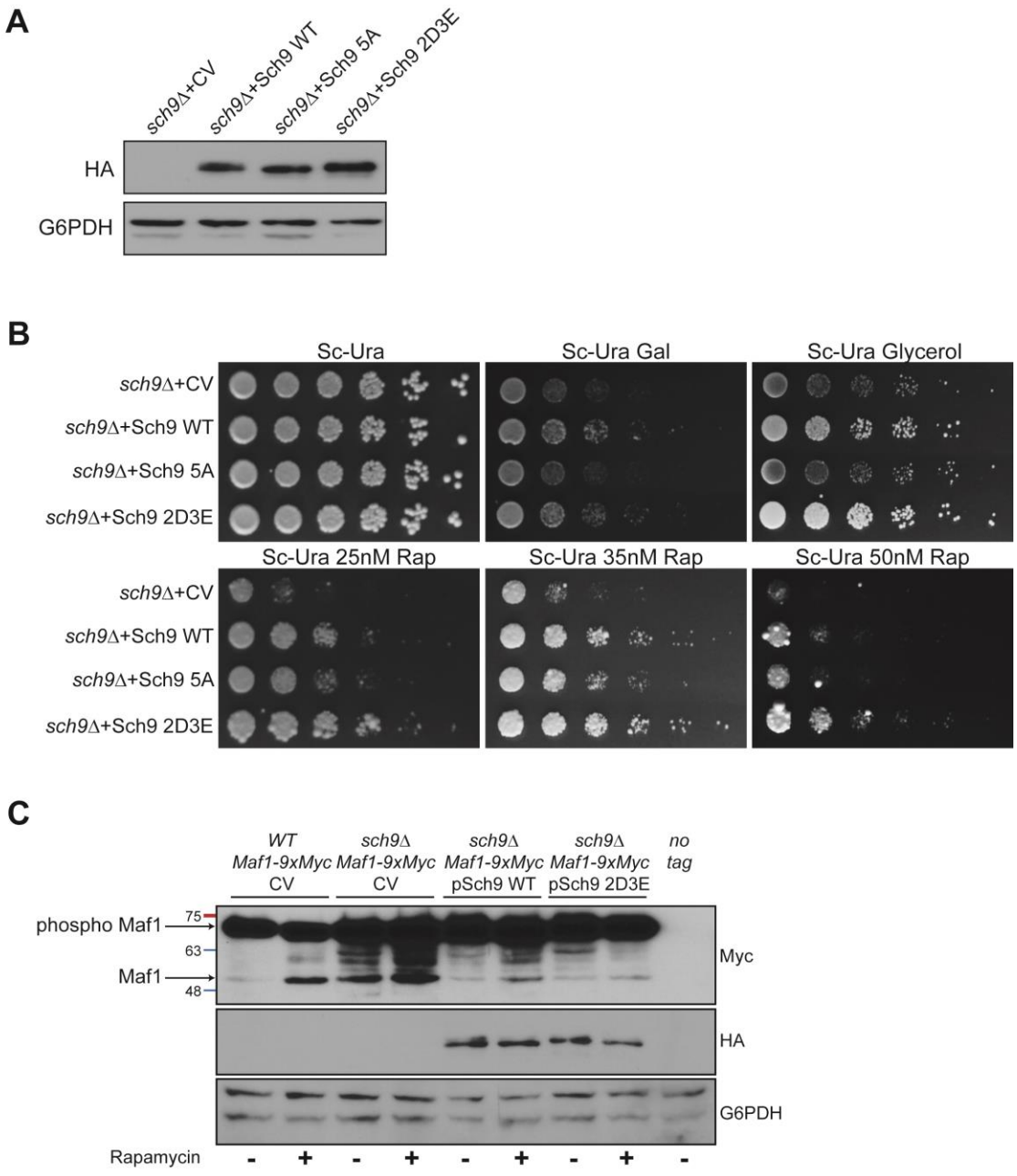

Figure S2

Figure S2. Control experiments for mutant Sch9 plasmids. (A) *sch9Δ* cells transformed with control vector (CV), wild-type Sch9 ($pSch9^{WT}$), and mutant forms where Sch9 activity is no longer

responsive to TORC1 (pSch9^{5A} and pSch9^{2D3E}) were grown to log phase in selective media. Whole-cell extracts were prepared and analyzed by immunoblot as indicated. (B) Strains from (A) were grown to saturation, five-fold serially diluted, and spotted onto the indicated plate media. (C) WT Maf1-9xMyc cells were transformed with CV, while the Maf1-9xMyc *sch9Δ* strain was transformed with CV, pSch9^{WT} and pSch9^{2D3E}. Cells were grown to log phase and then mock or 300nM rapamycin treated for 60 minutes. Extracts were prepared, resolved on 8% SDS-PAGE, and immunoblotted as shown.

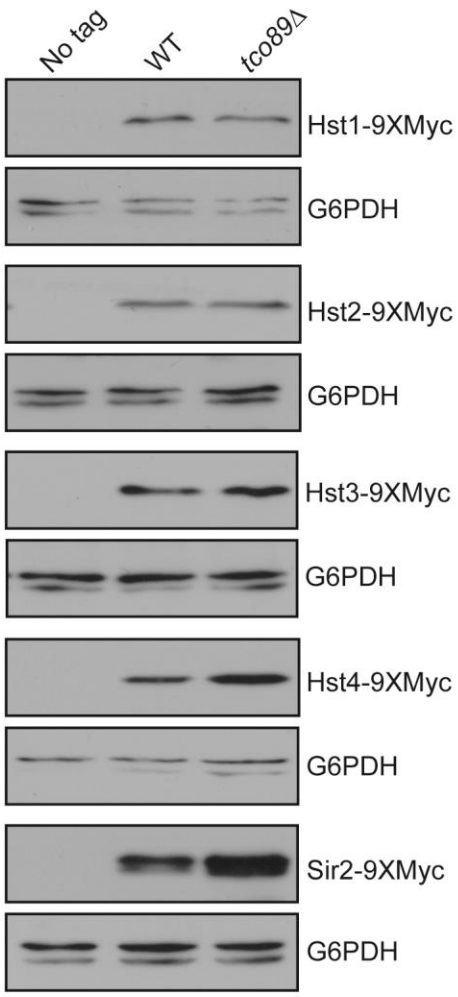
No tag
WT
tco89Δ
Hst1-9XMyc
G6PDH
Hst2-9XMyc
G6PDH
Hst3-9XMyc
G6PDH
Hst4-9XMyc
G6PDH
Sir2-9XMyc
G6PDH

Figure S3

Figure S3. Sirtuin protein levels in response to TORC1 inhibition. Representative immunoblots of no tag control, and WT or *tco89Δ* cells expressing the 9xMyc epitope-tagged sirtuins. Data shown is representative of at least 3 independent biological replicates.

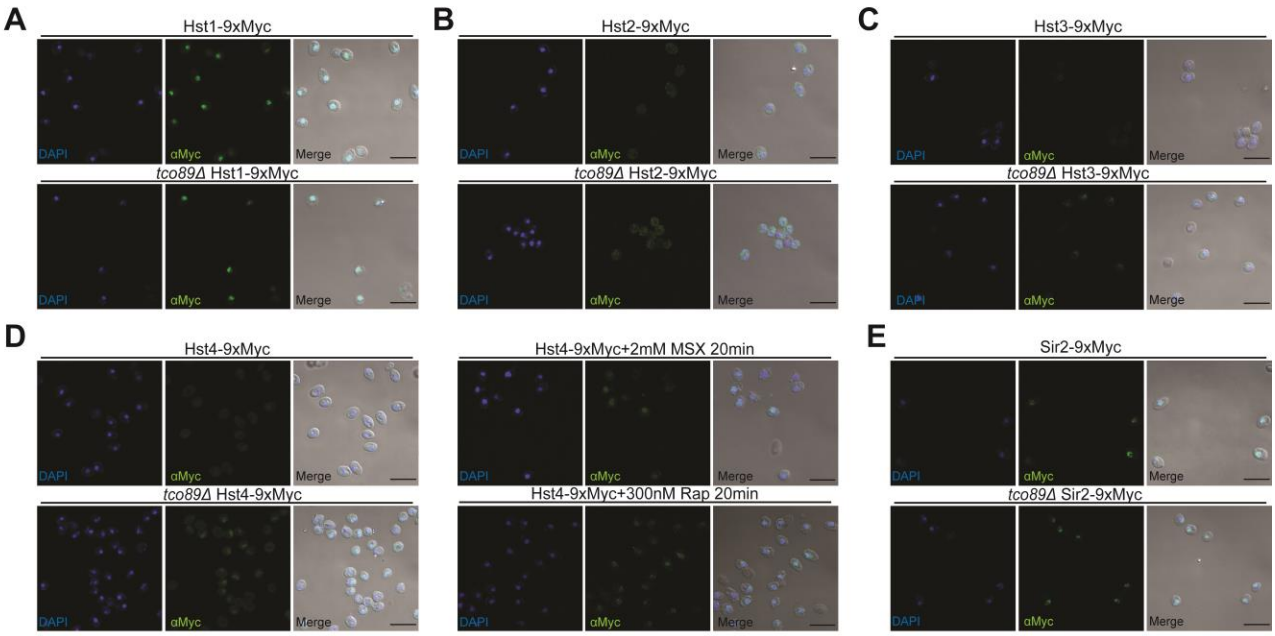

Figure S4

Figure S4. Sirtuin subcellular localization in response to TORC1 inhibition. (A-E) No tag control, and WT or *tco89Δ* cells expressing the 9xMyc epitope-tagged sirtuins were cultured to log phase, treated as indicated, and imaged by indirect immunofluorescence as described in the methods. Images are representative of at least three independent biological replicates, and are a subset of the quantification shown in Figure 6B and 6C.

Table 1. Yeast strains.

Strain	Genotype	Source
BY4741	MATa *his3Δ1 leu2Δ0 met15Δ0 ura3Δ0* BY4741	OPEN Bio
tco89Δ	BY4741; *tco89Δ::KanMX*	OPEN Bio
sch9Δ	BY4741; *sch9Δ::KanMX*	OPEN Bio
pnc1Δ	BY4741; *pnc1Δ::KanMX*	OPEN Bio
rpd3Δ	BY4741; *rpd3Δ::KanMX*	OPEN Bio
hda1Δ	BY4741; *hda1Δ::KanMX*	OPEN Bio
gln3Δ	BY4741; *gln3Δ::KanMX*	OPEN Bio
gat1Δ	BY4741; *gat1Δ::KanMX*	OPEN Bio
ure2Δ	BY4741; *ure2Δ::KanMX*	OPEN Bio
tpd3Δ	BY4741; *tpd3Δ::KanMX*	OPEN Bio
ppg1Δ	BY4741; *ppg1Δ::KanMX*	OPEN Bio
pph3Δ	BY4741; *pph3Δ::KanMX*	OPEN Bio
sit4Δ	BY4741; *sit4Δ::KanMX*	OPEN Bio
sap4Δ	BY4741; *sap4Δ::KanMX*	OPEN Bio
sap155Δ	BY4741; *sap155Δ::KanMX*	OPEN Bio
sap185Δ	BY4741; *sap185Δ::KanMX*	OPEN Bio
sap190Δ	BY4741; *sap190Δ::KanMX*	OPEN Bio
YNL387	MATa *his3Δ1 leu2Δ0 met15Δ0 ura3Δ0* BY4741 *tco89Δ::KanMX hst3Δ::NAT*	(CHEN *et al.* 2013)
YNL389	MATa *his3Δ1 leu2Δ0 met15Δ0 ura3Δ0* BY4741 *tco89Δ::KanMX hst4Δ::NAT*	(CHEN *et al.* 2012)
Y3033	W303-1A *tap42*Δ::*HIS3* pRS414-*TAP42*	(CHEN *et al.* 2012)
Y3032	W303-1A *tap42*Δ::*HIS3* pRS415-*tap42-11*	(YORIMITSU *et al.* 2009)
Y3035	W303-1A *tap42*Δ::*HIS3* pRS414-*tap42-109*	(YORIMITSU *et al.* 2009)
Y3034	W303-1A *tap42*Δ::*HIS3* pRS414-*tap42-106*	(YORIMITSU *et al.* 2009)
YNL541	MATa *his3Δ1 leu2Δ0 met15Δ0 ura3Δ0* BY4741 *tco89Δ::HphNT1 hst3Δ::KanMX*	This Study
YNL622	MATa *his3Δ1 leu2Δ0 met15Δ0 ura3Δ0* BY4741 *tco89Δ::NAT sit4Δ::KanMX*	This Study
YNL487	MATa *his3Δ1 leu2Δ0 met15Δ0 ura3Δ0* BY4741 *tco89Δ::NAT*	This Study
YNL516	MATa *his3Δ1 leu2Δ0 met15Δ0 ura3Δ0* BY4741 *tco89Δ::NAT hst1Δ::KanMX*	This Study
YNL519	MATa *his3Δ1 leu2Δ0 met15Δ0 ura3Δ0* BY4741 *tco89Δ::NAT hst2Δ::KanMX*	This Study
YNL517	MATa *his3Δ1 leu2Δ0 met15Δ0 ura3Δ0* BY4741 *tco89Δ::NAT sir2Δ::KanMX*	This Study

YNL502	MATa *his3Δ1 leu2Δ0 met15Δ0 ura3Δ0* BY4741 *tco89Δ::NAT rpd3Δ::KanMX*	This Study
YNL670	MATa *his3Δ1 leu2Δ0 met15Δ0 ura3Δ0* BY4741 *tco89Δ::NAT hda1Δ::KanMX*	This Study
YNL678	MATa *his3Δ1 leu2Δ0 met15Δ0 ura3Δ0* BY4741 *Hst1-9xMyc::KanMX*	This Study
YNL681	MATa *his3Δ1 leu2Δ0 met15Δ0 ura3Δ0* BY4741 *tco89Δ::NAT Hst1-9xMyc::KanMX*	This Study
YNL685	MATa *his3Δ1 leu2Δ0 met15Δ0 ura3Δ0* BY4741 *Hst2-9xMyc::KanMX*	This Study
YNL700	MATa *his3Δ1 leu2Δ0 met15Δ0 ura3Δ0* BY4741 *tco89Δ::NAT Hst2-9xMyc::KanMX*	This Study
YNL698	MATa *his3Δ1 leu2Δ0 met15Δ0 ura3Δ0* BY4741 *Hst3-9xMyc::KanMX*	This Study
YNL676	MATa *his3Δ1 leu2Δ0 met15Δ0 ura3Δ0* BY4741 *tco89Δ::NAT Hst3-9xMyc::KanMX*	This Study
YNL612	MATa *his3Δ1 leu2Δ0 met15Δ0 ura3Δ0* BY4741 *Hst4-9xMyc::KanMX*	This Study
YNL614	MATa *his3Δ1 leu2Δ0 met15Δ0 ura3Δ0* BY4741 *tco89Δ::NAT Hst4-9xMyc::KanMX*	This Study
YNL687	MATa *his3Δ1 leu2Δ0 met15Δ0 ura3Δ0* BY4741 *Sir2-9xMyc::KanMX*	This Study
YNL689	MATa *his3Δ1 leu2Δ0 met15Δ0 ura3Δ0* BY4741 *tco89Δ::NAT Sir2-9xMyc::KanMX*	This Study
YNL716	MATa *his3Δ1 leu2Δ0 met15Δ0 ura3Δ0* BY4741 *Hst4-9xMyc::HYGRO sit4Δ::KANMX*	This Study
YNL718	MATa *his3Δ1 leu2Δ0 met15Δ0 ura3Δ0* BY4741 *Hst4-9xMyc::HYGRO sit4Δ::KANMX tco89Δ:HphNT1*	This Study
YNL775	MATa *his3Δ1 leu2Δ0 met15Δ0 ura3Δ0* BY4741 *Hst4-9xMyc::KANMX sap4Δ::HYGRO*	This Study
YNL776	MATa *his3Δ1 leu2Δ0 met15Δ0 ura3Δ0* BY4741 *Hst4-9xMyc::KANMX sap4Δ::HYGRO tco89Δ::NAT*	This Study
YNL778	MATa *his3Δ1 leu2Δ0 met15Δ0 ura3Δ0* BY4741 *Maf1-9xMyc::NAT*	This Study
YNL780	MATa *his3Δ1 leu2Δ0 met15Δ0 ura3Δ0* BY4741 *Maf1-9xMyc::NAT sch9Δ KANMX*	This Study

Table 2. Yeast plasmids.

Parent Plasmid	Plasmid Description	Source
pADH TCO89-MYC	$ADH1_{prom}$TCO89-MYC; *URA3; CEN6/ARS*	This study
pADH SIT4-FLAG	$ADH1_{prom}$SIT4-FLAG; *URA3; CEN6/ARS*	This study
pRS416	*CEN6; ARS4; URA3*	(BRACHMANN *et al.* 1998)
pJU677	pRS416; SCH9-6xHA	(URBAN *et al.* 2007)
pJU790	pRS416; SCH9-6xHA (T723A, S726A, T737A, S758A, S765A)	(URBAN *et al.* 2007)
pJU855	pRS416; SCH9-6xHA (T723D, S726D, T737E, S758E, S765E)	(URBAN *et al.* 2007)